Supplementary Information for:

Excitation-wavelength-dependent organic photoluminescence molecule with high quantum yield integrating both ESIPT and PCET mechanisms

Mengyuan Song,[a,d] Meng Liu,[b] Xue Zhang,[c] Haijuan Qin,[e] Jinglu Sun,[f,d] Juanjuan Wang,[d,*] Qian Peng,[d] Zhiwei Zhao,[g] Guohui Zhao,[b] Xianchang Yan,[b,d] Yongxin Chang,[a] Yahui Zhang,[a] Dongdong Wang,[a] Junhui Wang,[b,d,*] Jianzhang Zhao,[c,*] and Guangyan Qing[a,d,*]

[a] State Key Laboratory of Medical Proteomics, National Chromatographic R. & A. Center, CAS Key Laboratory of Separation Science for Analytical Chemistry, Dalian Institute of Chemical Physics, Chinese Academy of Sciences, Dalian 116023, P. R. China
[b] State Key Laboratory of Molecular Reaction Dynamics, Dalian Institute of Chemical Physics, Chinese Academy of Sciences, Dalian 116023, P. R. China
[c] State Key Laboratory of Fine Chemicals, Frontiers Science Centre for Smart Materials, School of Chemical Engineering, Dalian University of Technology, Dalian 116024, P. R. China
[d] University of Chinese Academy of Sciences, Beijing 100049, P. R. China
[e] Research Centre of Modern Analytical Technology, Tianjin University of Science and Technology, Tianjin 300457, P. R. China
[f] Key Laboratory of Chemical Lasers, Dalian Institute of Chemical Physics, Chinese Academy of Sciences, Dalian 116023, P. R. China
[g] Laboratory of Advanced Spectroelectrochemistry and Li-ion Batteries, Dalian Institute of Chemical Physics, Chinese Academy of Sciences, Dalian 116023, P. R. China
[†]These authors contributed equally
*Corresponding authors: jjwang@ucas.ac.cn, zhaojzh@dlut.edu.cn, wjh@dicp.ac.cn, qinggy@dicp.ac.cn

Contents

1. Materials and Characterization

Materials: Salicylaldehyde, 5-methylsalicylaldehyde, 2-aminothiophenol, 2-hydroxy-4-methylbenzaldehyde, tetrabutylammonium hexafluorophosphate ($Bu_4N[PF_6]$), L-histidine, histamine, L-tryptophan, hexamethylenetetramine (HMTA), and sodium deuteroxide (NaOD, 40 wt% in D_2O, 99.5 atom % D) were purchased from Shanghai Aladdin Biochemical Technology Co., Ltd. Methanol-d_4 (99.8 atom % D) and dimethyl sulfoxide-d_6 (DMSO-d_6, 99.8 atom % D, with 0.03% (v/v) tetramethylsilane (TMS)) were purchased from Beijing Inno-Chem Science & Technology Co., Ltd. Chloroform-*d* ($CDCl_3$, 99.8 atom % D, containing 0.03% v/v TMS and stabilized with silver foil) was purchased from J&K Scientific. Dimethyl sulfoxide (DMSO, 99.7%, Water≤50 ppm) used in the spectroelectrochemical experiments, and 5-tert-butyl-2-hydroxybenzaldehyde were purchased from Shanghai Jizhi Biochemical Technology Co., Ltd. Methanol (CH_3OH) used in the test was of spectrally pure grade and purchased from Shanghai Boer Chemical Reagent Co., Ltd. Other solvents and reaction reagents, including CH_3OH, silver nitrate ($AgNO_3$), trifluoroacetic acid (TFA), Triethylamine (TEA), iodine (I_2), hydrogen peroxide (H_2O_2, 30 wt% solutions in water), hydrochloric acid (HCl, 37 wt% solutions in water), sodium hydroxide (NaOH), petroleum ether, ethyl acetate and dichloromethane (CH_2Cl_2) were purchased from Sinopharm Chemical Reagent Co., Ltd. (P. R. China). All chemicals were used as received, without further purification.

Characterization: Hydrogen and carbon nuclear magnetic resonance (^1H, ^{13}C NMR) spectra were obtained using a Bruker AVANCE III 400-MHz or AVANCE III HD 700-MHz spectrometer (Bruker Corp., Germany). The sample was purified by high performance liquid chromatography (HPLC) to obtain the target product. The separation process was performed using a 10 mm × 250 mm column filled with C18 silica gel stationary phase (5 μm, 100 Å). A binary gradient elution was performed at room temperature with a flow rate of 3 $mL \cdot min^{-1}$, with eluent A consisting of ultrapure water (H_2O) and eluent B comprising CH_3OH plus 0.1% TEA (v/v). Detection was performed using a UV/visible (UV-Vis) absorbance detector with wavelengths of 254 and 320 nm. The eluate obtained from separation was identified using mass spectrometry and subsequently freeze-dried. Mass spectra (MS) were recorded on an Agilent 6540 Quadrupole Time-of-Flight (Q-TOF) mass spectrometer (Agilent, USA). Steady-state absorption spectra were measured with a Perkin-Elmer Lamda-365 Ultraviolet-visible (UV-vis) spectrophotometer. Fluorescence spectra were measured using a Perkin-Elmer FL 6500 fluorescence spectrometer (PerkinElmer, USA) and an Edinburgh FLS 1000 spectrometer (Edinburgh Instruments, UK). Temperature-dependence of all photoluminescence (PL) spectra was recorded on an Edinburgh FLS 1000 spectrofluorometer. Temperature-dependent UV-visible absorption spectra were obtained using an Agilent Cary 60 UV-vis spectrophotometer. Nanosecond transient absorption (TA) spectra were measured using an LP980 laser flash photolysis spectrometer (Edinburgh Instruments, UK). Scanning electron microscopy (SEM) images were carried out on a FlexSEM 1000 II instrument. In the spectroelectrochemical experiments, cyclic voltammetry curves were recorded with a CHI610D electrochemical workstation (CHI instruments, Inc., Shanghai, P. R. China). UV-Vis spectra were recorded with an Agilent 8453 UV-vis spectroscopy system (Agilent Technologies Inc., USA). Infrared spectroscopy measurements were conducted on a Thermofisher Scientific Nicolet iS50 spectrometer (USA) equipped with a liquid nitrogen-cooled MCT-B detector at room temperature.

Absolute quantum yield was obtained on an Edinburgh Instrument FLS980 Integrating sphere. The phosphorescence lifetime was measured using the Triggered-Accumulation multi-channel scaler (MSC) mode in the time-correlated single photon counting (TCSPC) system (SPC-150, Becker & Hickl GmbH, Germany). Excitation of the sample was achieved with a pulsed 375 nm laser (PDL 800-B, PicoQuant, Germany), and the phosphorescence photons were collected by a high-speed detector (HPM-100-50, Hamamatsu, Japan).

2. Method

Preparation of NMR Samples

The solutions for recorder of the ^{1}H and ^{13}C spectra NMR of compounds **3** and **4** were prepared by dissolving 26 mg of powder sample in 0.5 mL of a mixed solution of Methanol-d_4: NaOD=10: 1.

Femtosecond Transient Absorption (fs-TA) Spectra

The femtosecond pump-probe transient absorption (TA) measurements were performed using a regenerative amplified Ti: sapphire laser system (Coherent; 800 nm, 70 fs, 6 mJ/pulse, and 1 KHz repetition rate) as the laser source, along with a femto-TA100 spectrometer (Time-Tech Spectra, P. R. China). Briefly, the 800 nm output pulse from the regenerative amplifier was split in two parts with a 50% beam splitter. The transmitted part was used to pump a TOPAS Optical Parametric Amplifier (OPA), which generated a wavelength-tunable laser pulse from 250 nm to 2.5 μm as pump beam. The reflected 800 nm beam was subsequently split again into two parts, one part with less than 10% was attenuated with a neutral density filter and focused into a 2 mm thick sapphire window to generate a white light continuum (WLC) used for probe beam. The probe beam was focused onto the sample with an aluminum parabolic reflector. After interacting with the sample, the probe beam was collimated and then focused into a fiber-coupled spectrometer equipped with CMOS sensors, detecting at a frequency of 1 KHz. The intensity of the pump pulse used in the experiment was controlled by a variable neutral-density filter wheel, with the delay between the pump and probe pulses was controlled by a motorized delay stage. The pump pulses were chopped by a synchronized chopper at 500 Hz, and the absorbance change was calculated using two adjacent probe pulses (pump-blocked and pump-unblocked).[1]

The temperature during all experiments was controlled using a Blue Haike's cryostat. All samples were maintained at the target temperature for 30 min before the testing to ensure the stability. The global fitting and target analysis were carried with a sequential model using the software Glotaran.

Nanosecond Transient Absorption (ns-TA) Spectra

Ns-TA spectra were measured on an LP980 laser flash photolysis spectrometer (Edinburgh Instruments, UK). The signal was digitized using a Tektronix MDO 3022 oscilloscope, and all samples were degassed with N_2 for approximately 15 min prior to measurement.

Kinetic fitting and life calculation formula

Data analysis used either a single-exponential (Eq. 1) or double-exponential function (Eq. 2), performed with a software package provided by the Originpro 2021:[2]

$$y = Ae^{-t/\tau} \quad (1)$$

$$y = A_1 e^{-t/\tau_1} + A_2 e^{-t/\tau_2} \quad (2)$$

Where A_1, A_2 are the pre-exponential factors, and τ_1, τ_2 correspond to the decay time constants.

For double-exponential fitting, the average lifetime (τ) was calculated using the following equation (Eq. 3):

$$\tau = \frac{A_1\tau_1^2 + A_2\tau_2^2}{A_1\tau_1 + A\tau_2} \quad (3)$$

UV-vis spectroelectrochemistry

Cyclic voltammetry curves were recorded using a CHI610D electrochemical workstation (CHI instruments, Inc., Shanghai, P. R. China). The counter electrode was a platinum electrode, while a glassy carbon (GC) electrode served as the working electrode. Spectroelectrochemistry was performed in a quartz electrochemical cell with a path length of 0.1 cm. A platinum gauze worked as the working electrode, and a platinum wire was the counter electrode. The potential was regulated using the CHI610D electrochemical workstation, and the spectra were recorded with an Agilent 8453 UV-vis spectroscopy system (Agilent Technologies Inc., USA). In both cases, $Bu_4N[PF_6]$ was used as the supporting electrolyte, and the $Ag/AgNO_3$ (0.1 M in DMSO) couple served as the reference electrode. Samples were deaerated with N_2 for approximately 15 min before measurement, and the N_2 atmosphere was maintained during the measurements.[3]

***In situ* FT-IR measurements**

In situ FT-IR measurements with external reflection configuration were conducted using a Spectroelectrochemistry Partners SP-02 cell mounted on an attenuated total reflection (ATR) accessory (Pike MIRacle, Netherlands and Belgium) fitted with a single-bounce silicon top plate. The SP-02 cell contained a GC working electrode (diameter 3 mm), a platinum counter electrode, and a silver wire reference electrode. All measurements were conducted on a Thermofisher Scientific Nicolet iS50 spectrometer (USA), equipped with a liquid nitrogen-cooled MCT-B detector at room temperature. The spectra results were collected at selected potentials with a resolution of 4 cm^{-1}. All the spectra are presented in the absorbance units defined as $\log(R/R_0)$, where R and R_0 represent the IR signal at the potential of interest and open circuit potential (OCP), respectively. High purity N_2 (99.999%) was used to exclude air from the optical path throughout the experiments.[4]

Preparation of 2-PVA film composite membrane

5 mg of compound **2** were dissolved in 500 μL of CH_3OH. This solution was added to a 10 mL of 5 wt% PVA aqueous solution stirring magnetically until a transparent solution. The mixture (5 mL) into a plastic petri dish with a diameter of 35 mm and placed in an oven at 60 °C for 6 h to dry it into a film. The film was cut into the desired shape.

Test of Photoluminescence Quantum Yield of PVA Film

Absolute quantum yield was obtained on an Edinburgh Instrument FLS980 Integrating sphere. The excitation light was set at 363 nm and 396 nm to obtain their absolute quantum yields, respectively.

Phosphorescence life test of PVA film

The phosphorescence lifetime was measured using the Triggered-Accumulation multi-channel scaler (MCS) mode in the time-correlated single photon counting (TCSPC) system (SPC-150, Becker & Hickl GmbH, Germany). Excitation of the sample was achieved with a pulsed 375 nm laser (PDL 800-B, PicoQuant, Germany), and the phosphorescence photons were collected by a high-speed detector (HPM-100-50, Hamamatsu, Japan).

DFT calculations

Density function theory (DFT) and time-dependent DFT (TD-DFT) calculations were performed to simulate the ESIPT process of **2**, and the photophysical properties of the species where the proton migrates from the HBT moiety to the imidazole group. All geometry optimizations were conducted at the B3LYP/6-31G* level using the Gaussian 16 software package[5]. The polarizable continuum model (PCM) was employed to account for solvent effects in methanol (CH_3OH). The optimized structures were verified to exhibit no imaginary frequencies, confirming their ground or excited state minima. Zero-point vibrational energy corrections were applied without scaling.

3 Synthesis and characterization

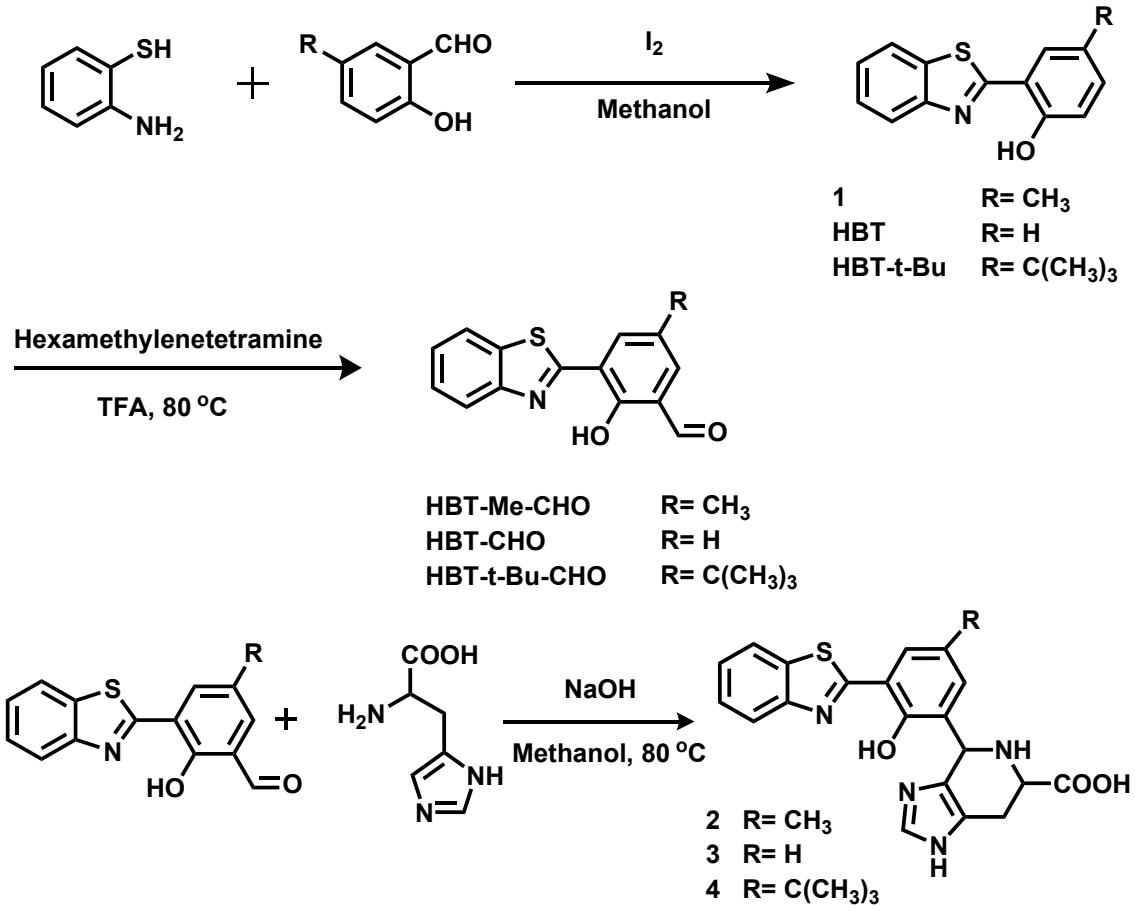

Scheme S1. Synthetic routes to compound of **2, 3,** and **4.**

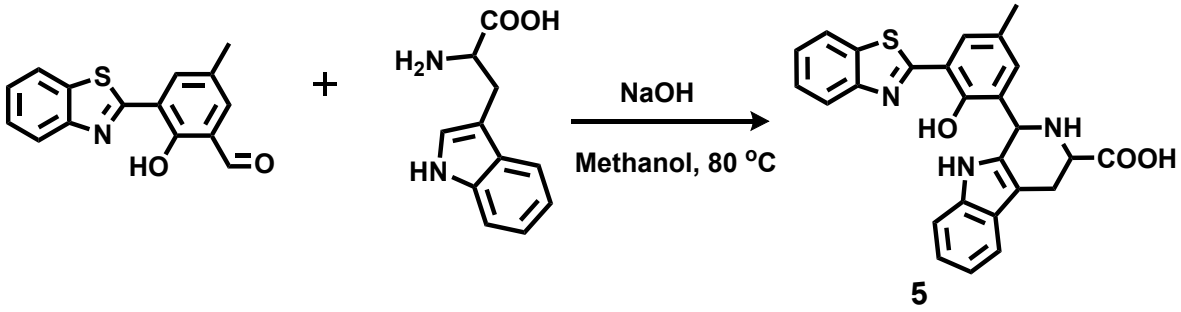

Scheme S2. Synthetic route to compound of **5.**

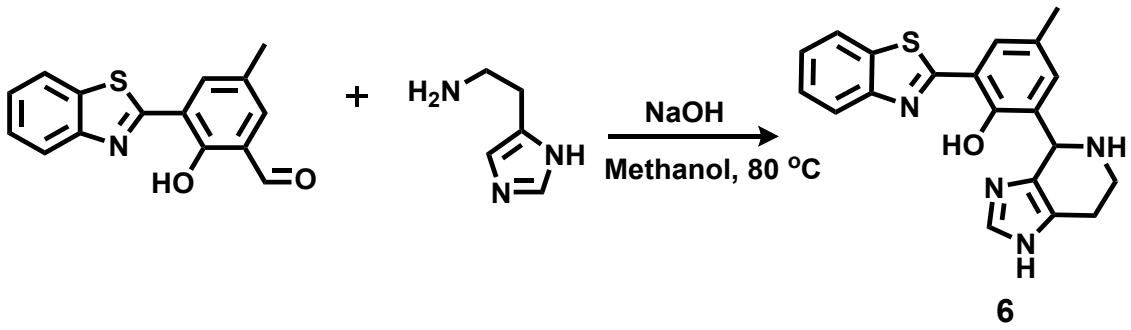

Scheme S3. Synthetic route to compound of **6.**

Synthesis of 2-(2-Hydroxy-3-formyl-5-methylphenyl)benzothiazole (HBT-Me-CHO)[6]

In a 100 mL round-bottom flask, a solution of 2-aminobenzenethiol (1.09 g, 10 mmol) and 2-hydroxy-5-methylbenzaldehyde (1.36 g, 10 mmol) in anhydrous CH_3OH (30 mL) was added with I_2 (0.25 g, 1 mmol). The mixture was stirred at room temperature, and after approximately 5 minutes, a white precipitate began to form. The reaction mixture was further stirred for another 5 h. The solid was collected by filtration, washed with cold CH_3OH, and recrystallized from CH_3OH. The crude product was then purified by silica gel column chromatography, using a petroleum ether and ethyl acetate mixture (50: 1, v/v) as the eluent, yielding pure 2-(2-Hydroxy-5-methylphenyl)benzothiazole (1) as a white solid (510 mg, yield: 21%). ^{1}H NMR (400 MHz, DMSO-d_6): δ (ppm): 11.37 (s, 1H), 8.15–8.10 (m, 1H), 8.05 (dt, J_1 = 8.2 Hz, J_2 =0.9 Hz, 1H), 7.96 (dd, J_1 = 2.3 Hz, J_1 =0.9 Hz, 1H), 7.53 (ddd, J_1 = 8.2 Hz, J_2 = 7.1 Hz, J_3 =1.3 Hz, 1H), 7.43 (ddd, J_1 = 8.2 Hz, J_2 = 7.2 Hz, J_3 = 1.2 Hz, 1H), 7.21 (dd, J_1 = 8.4 Hz, J_2 = 2.3 Hz, 1H), 6.98 (d, J = 8.4 Hz, 1H), 2.31 (s, 3H). ^{13}C NMR (400 MHz, DMSO-d_6): δ (ppm): 165.35, 154.21, 151.46, 134.23, 133.23, 128.40, 128.27, 126.43, 125.01, 122.04, 121.89, 117.89, 116.87, 20.02. MS (ESI): Calcd. for $C_{14}H_{11}NOS$ $[M+H]^+$ 242.0634, found 242.0639.

In a 100 mL round bottomed flask, 1 (241 mg, 1 mmol) was dissolved in 10 mL of TFA, and then HMTA (168 mg, 1.2 mmol) was added. The solution was refluxed for 12 h and then allowed to cool to room temperature. The reaction mixture was poured into 30 mL of 6 M HCl and extracted with CH_2Cl_2. The combined organic layers were washed with saturated brine. The crude product was then purified by silica gel column chromatography (ethyl acetate: petroleum ether = 50: 1 to 10: 1, v: v), yielding pure compound HBT-Me-CHO as a yellow solid (235 mg, yield: 87%). ^{1}H NMR (400 MHz, $CDCl_3$) δ(ppm): 12.99 (s, 1H), 10.48 (s, 1H), 8.01 (d, J = 8.1 Hz, 1H), 7.92 (dd, J_1 = 8.0 Hz, J_2 =1.2 Hz, 1H), 7.86 (s, 1H), 7.68 (d, J = 2.3 Hz, 1H), 7.53 (t, J = 8.44 Hz, 1H), 7.43 (t, J = 8.20 Hz, 1H), 2.39 (s, 3H). ^{13}C NMR (400 MHz, $CDCl_3$) δ(ppm): 190.88, 158.54, 151.55, 135.14, 133.16, 132.53, 128.91, 126.86, 125.82, 123.76, 122.40, 121.59, 118.70, 29.72, 20.33. MS (ESI): Calcd. for $C_{15}H_{11}NO_2S$ $[M+H]^+$ 270.0583, found 270.0585.

Synthesis of 3-(benzo[d]thiazol-2-yl)-2-hydroxybenzaldehyde (HBT-CHO)[7]

In a 100 mL round-bottom flask, 30 mL of CH_3OH was added along with 1.25 g of 2-aminothiophenol (10 mmol) and 1.28 g of salicylaldehyde (10.5 mmol). The mixture was stirred for 30 min, during which yellow solids began to form. Then, a mixed solution containing 2 mL of concentrated HCl and 4 mL of 30% H_2O_2, was added dropwise with constant stirring. The mixture was stirred at room temperature for 5 h, resulting in the formation of a brown precipitate. The precipitate was filtered, washed with CH_3OH, and recrystallized from CH_3OH. The crude product was further purified by silica gel column chromatography, using a petroleum ether and ethyl acetate mixture (50: 1, v/v) as the eluent, yielding pure 2-(2-Hydroxyphenyl)benzothiazole (HBT) as a white solid (0.7 g, yield: 31%). ^{1}H NMR (400 MHz, DMSO-d_6) δ(ppm): δ 11.61 (s, 1H), 8.15 (ddd, J_1 = 13.1 Hz, J_2 = 8.0 Hz, J_3 = 1.5 Hz, 2H), 8.06 (d, J = 8.1 Hz, 1H), 7.54 (ddd, J_1 = 8.2 Hz, J_2 = 7.1 Hz, J_3 = 1.3 Hz, 1H), 7.49–7.38 (m, 2H), 7.09 (dd, J_1 = 8.2 Hz, J_2 = 1.1 Hz, 1H), 7.05–6.98 (m, 1H). ^{13}C NMR (400 MHz, DMSO-d_6) δ(ppm): 165.28, 156.28, 151.43, 134.21, 132.47, 128.52, 126.46, 125.09, 122.11, 121.99, 119.75, 118.30, 116.97. MS (ESI): Calcd. for $C_{13}H_9NOS$ $[M+H]^+$ 228.0478, found 228.0474.

In a 100 mL round bottomed flask, 1.14 g of HBT (5 mmol) and 0.77 g of HMTA (5.5 mmol) were mixed, and 10 mL of TFA was added with stirring. The solution was refluxed for 12 h, followed by cooling to room temperature. The reaction mixture was poured into 30 mL of 6 mol· L^{-1} HCl and extracted with CH_2Cl_2. The combined organic layers were washed with saturated brine. The crude product was then purified by silica gel column chromatography (ethyl acetate: petroleum ether = 50: 1–10: 1, v: v), yielding pure HBT-CHO as a yellow solid (0.21 g, yield: 16%). ^{1}H NMR (400 MHz, $CDCl_3$) δ(ppm): 13.22 (s, 1H), 10.50 (s, 1H), 8.10–7.93 (m, 2H), 7.87 (ddd, J_1 = 11.2 Hz, J_2 = 7.8 Hz, J_3 = 1.5 Hz, 2H), 7.51 (td, J_1 = 8.2 Hz, J_2 = 7.7 Hz, J_3 = 1.3 Hz, 1H), 7.42 (td, J_1= 7.6 Hz, J_2 =7.2 Hz, J_3 =1.2 Hz, 1H), 7.02 (t, J = 7.7 Hz, 1H). ^{13}C NMR (400 MHz, $CDCl_3$) δ(ppm): 190.55, 160.57, 151.51, 134.63, 133.09, 132.14, 131.21, 127.00, 126.02, 124.19, 122.49, 121.68, 119.54, 118.09. MS (ESI): Calcd. for $C_{14}H_9NO_2S$ $[M+H]^+$ 256.0427, found 256.0424.

Synthesis of 3-(benzo[d]thiazol-2-yl)-5-(tert-butyl)-2-hydroxybenzaldehyde (HBT-t-Bu-CHO)

The synthesis method of compound 2-(2-Hydroxy-5-(tert-butyl)phenyl)benzothiazole (HBT-t-Bu) is similar to that of compound HBT. 5-tert-butyl-2-hydroxybenzaldehyde (1.78 g, 10 mmol) and 2-aminobenzenethiol (1.09 g, 10 mmol) were added in anhydrous CH_3OH (30 mL). The mixture was stirred for 30 min. Then, a mixed solution containing 2 mL of concentrated HCl and 4 mL of 30% H_2O_2, was added dropwise with constant stirring. The mixture was stirred at room temperature for 5 h to obtain HBT-t-Bu. The product was isolated as a white solid (0.82 g, yield: 28.9%). ^{1}H NMR (400 MHz, $CDCl_3$) δ(ppm): 11.34 (s, 1H), 8.14 (d, J = 2.5 Hz, 1H), 8.12 (dt, J_1 = 7.7 Hz, J_1 = 1.0 Hz, 1H), 8.07 (dt, J_1 = 8.1 Hz, J_2 = 0.9 Hz, 1H), 7.53 (ddd, J_1 = 8.3 Hz, J_2 = 7.2 Hz, J_1 = 1.3 Hz, 1H), 7.49–7.39 (m, 2H), 7.03 (d, J = 8.6 Hz, 1H), 1.31 (s, 9H). ^{13}C NMR (400 MHz, $CDCl_3$) δ(ppm):

165.31, 154.15, 151.49, 141.81, 134.38, 129.85, 126.36, 124.92, 124.28, 122.11, 121.92, 117.60, 116.74, 33.89, 31.21. MS (ESI): Calcd. for $C_{17}H_{17}NOS$ $[M+H]^+$ 284.1104, found 284.1112.

HBT-t-Bu (0.4 g, 1.4 mmol) and HMTA (0.26 g, 1.8 mmol) in TFA (10 mL) stirred at 80 °C for 12 h were converted to HBT-t-Bu-CHO. The product was isolated as a white solid (0.33 g, yield: 75.5%). ^{1}H NMR (400 MHz, DMSO-d_6) δ(ppm): 12.65 (s, 1H), 10.32 (s, 1H), 8.54–8.30 (m, 1H), 8.16 (dd, J_1 = 23.0 Hz, J_1 =8.1 Hz, 2H), 8.05–7.77 (m, 1H), 7.54 (dt, J_1 = 34.0 Hz, J_1 =7.5 Hz, 2H), 1.37 (s, 9H). ^{13}C NMR (400 MHz, DMSO-d_6) δ(ppm): 192.98, 164.57, 156.81, 151.08, 142.47, 133.89, 131.54, 130.38, 126.87, 125.73, 122.90, 122.41, 122.25, 119.27, 34.10, 30.94. MS (ESI): Calcd. for $C_{18}H_{17}NO_2S$ $[M+H]^+$ 312.1053, found 312.1056.

Synthesis of 2, 3, 4, 5, and 6[8]

2-(benzo[d]thiazol-2-yl)-6-(6-methyl-4,5,6,7-tetrahydro-1H-imidazo[4,5-c]pyridin-4-yl)phenol (2): HBT-Me-CHO (0.27 mg, 1.0 mmol) and L-histidine (0.23 mg, 1.5 mmol) was added to 30 mL of CH_3OH. NaOH (0.1 g, 2.5 mmol) was then added to the above solution and refluxed for 12 h. After cooling to room temperature, CH_3OH was removed by rotary evaporation and the residue was dissolved in an aqueous solution. The solution was neutralized to pH = 7 using HCl aqueous solution. The resulting precipitate was collected by filtration and washed three times with water. Finally, the product was freeze-dried, yielding 0.38 g of **2** as a yellow solid (yield: 93.6%). ^{1}H NMR (700 MHz, Methanol-d_4) δ(ppm): 7.97–7.93 (m, 2H, Benzothiazole, –C*H*–), 7.70 (s, 1H, 3-Phenol, –C*H*–), 7.53–7.44 (m, 2H, Benzothiazole, –C*H*–, Imidazole, –C*H*–), 7.38 (t, J = 7.8 Hz, 1H, Benzothiazole, –C*H*–), 7.20 (s, 1H, 5-Phenol, –C*H*–), 5.44 (s, 1H, –C*H*–N), 3.65 (dd, J_1 = 11.3 Hz, J_2 = 4.3 Hz, 1H, –C*H*–COOH), 3.08 (td, J_1 = 15.4 Hz, J_2 = 4.4 Hz, 1H, –CH_2–), 2.92–2.78 (m, 1H, –CH_2–), 2.30 (s, 3H, –CH_3). ^{13}C NMR (700 MHz, Methanol-d_4) δ(ppm): 178.67, 169.49, 156.42, 152.97, 136.37, 136.03, 135.55, 134.99, 134.60, 129.18, 129.00, 127.61, 126.34, 122.76, 122.67, 60.05, 56.92, 27.94, 20.64. MS (ESI): Calcd. for $C_{21}H_{18}N_4O_3S$ $[M+H]^+$ 407.1172, found $[M+H]^+$ 407.1173.

4-(3-(benzo[d]thiazol-2-yl)-2-hydroxyphenyl)-4,5,6,7-tetrahydro-1H-imidazo[4,5-c]pyridin-5-ium-6-carboxylate (3): The title compound was synthetized similarly to compound **2**. HBT-CHO (0.1 g, 0.4 mmol) and L-histidine (0.1 g, 0.64 mmol) reacted in CH_3OH (30 mL) stirred at room temperature for 12 h were converted to compound **3**. This reaction yielded 0.14 g of **3** as a yellow solid (yield: 89.3%). ^{1}H NMR (400 MHz, Methanol-d_4: NaOD = 10 : 1) δ(ppm): 8.06 (dd, J_1 = 8.1 Hz, J_2 = 1.9 Hz, 1H, Phenol, –C*H*–), 7.93–7.72 (m, 2H, Benzothiazole, –C*H*–), 7.50 (s, 1H, Imidazole, N–C*H*–N), 7.34 (td, J_1 = 8.0 Hz, J_2 = 7.6 Hz, J_3 = 2.5 Hz, 1H, Benzothiazole, –C*H*–), 7.21 (t, J = 7.5 Hz, 1H, Benzothiazole, –C*H*–,), 6.57–6.39 (m, 1H, Phenol, –C*H*–), 6.31 (t, J = 7.6 Hz, 1H, Phenol, –C*H*–), 5.71 (s, 1H, –C*H*–N), 3.44 (d, J_1 = 4.3 Hz, 1H, –C*H*–COOH), 3.00 (ddd, J_1 = 15.5 Hz, J_2 = 7.3 Hz, J_3 = 3.2 Hz, 1H, –CH_2–), 2.74 (tt, J_1 = 15.6 Hz, J_2 = 6.8 Hz, 1H, –CH_2–). ^{13}C NMR (400 MHz, Methanol-d_4: NaOD = 10 : 1) δ(ppm): 180.35, 169.10, 152.67, 136.65, 135.34, 134.75, 133.70, 133.51, 132.34, 131.94, 130.87, 127.81, 126.41, 124.23, 122.23, 121.27, 112.42, 60.79, 51.60, 28.65. MS (ESI): Calcd. for $C_{20}H_{16}N_4O_3S$ $[M+H]^+$ 393.1016, found 393.1015.

4-(3-(benzo[d]thiazol-2-yl)-5-(tert-butyl)-2-hydroxyphenyl)-4,5,6,7-tetrahydro-1H-imidazo[4,5-c]pyridin-5-ium-6-carboxylate (4)：Similarly, the title compound was synthetized using HBT-t-Bu-CHO (0.31 mg, 1 mmol) as a reactant with L-histidine (0.23 mg, 1.5 mmol), resulting in 0.4 g of **4** as a yellow solid (yield: 89.2%). ^{1}H NMR (400 MHz, Methanol-d_4: NaOD = 10 : 1) δ(ppm): 8.08–7.92 (m, 2H, Benzothiazole, –C*H*–), 7.84 (d, J = 2.4 Hz, 1H, 3-Phenol, –C*H*–), 7.72 (s, 1H), 7.59–7.51 (m, 1H, Benzothiazole, –C*H*–), 7.46 (t, J = 5.0 Hz, 1H, Benzothiazole, –C*H*–), 6.99 (d, J = 2.4 Hz, 1H, 5-Phenol, –C*H*–), 5.78 (s, 1H, –C*H*–N), 3.53 (dd, J_1 = 10.5 Hz, J_2 =4.6 Hz, 1H, –C*H*–COOH), 3.23–3.15 (m, 1H, –CH_2–), 3.19 (ddd, J_1 = 16.0 Hz, J_2 = 11.8 Hz, J_3 = 3.7 Hz, 1H, –CH_2–), 1.28 (s, 9H, –C(CH_3)$_3$). ^{13}C NMR (400 MHz, Methanol-d_4: NaOD = 10: 1) δ(ppm): 178.34, 170.96, 156.82, 153.67, 143.43, 142.68, 136.89, 135.17, 131.91, 129.50, 128.44, 127.18, 126.49, 126.03, 123.41, 122.67, 118.61, 56.32, 54.88, 32.29, 35.56, 27.49. MS (ESI): Calcd. for $C_{24}H_{24}N_4O_3S$ $[M+H]^+$ 449.1642, found 449.1649.

2-(benzo[d]thiazol-2-yl)-6-(2,3,4,4b,8a,9-hexahydro-1H-pyrido[3,4-b]indol-1-yl)-4-methylphenol (5)： Similarly, HBT-Me-CHO (0.27 mg, 1.0 mmol) and L-tryptophan (0.3 mg, 1.5 mmol) to produce 0.43 g of **5** as a yellow solid (yield: 94.5%). ^{1}H NMR (400 MHz, DMSO-d_6) δ(ppm): δ 10.39 (s, 1H, Indole, –N*H*–), 8.13–7.92 (m, 3H, Benzene ring, –C*H*–), 7.60–7.19 (m, 5H, Benzene ring, –C*H*–), 7.09–6.95 (m, 2H, Benzene ring, –C*H*–), 5.58 (s, 1H, –C*H*–N), 3.85 (dd, J_1 = 11.5 Hz, J_2 = 4.2 Hz, 1H, –C*H*–COOH), 3.22–3.15 (m, 1H, –CH_2–), 2.91 (t, J = 14.3, 1H, –CH_2–), 2.39 (s, 3H, –CH_3). ^{13}C NMR (400 MHz, DMSO-d_6) δ(ppm): 173.17, 165.15, 164.44, 154.89, 151.43, 136.53, 134.72, 133.11, 132.65, 131.59, 129.69, 124.78, 127.65, 127.39, 126.31, 122.00, 121.15, 118.72, 117.85, 111.38, 106.59 55.70, 51.53, 24.86, 20.39. MS (ESI): Calcd. for $C_{26}H_{21}N_3O_3S$ $[M+H]^+$ 456.1376, found 456.1389.

2-(benzo[d]thiazol-2-yl)-6-(6-methyl-4,5,6,7-tetrahydro-1H-imidazo[4,5-c]pyridin-4-yl)phenol (6): Histamine (0.17 mg, 1.5 mmol) was reacted with HBT-Me-CHO (0.27 mg, 1.0 mmol) to produce 0.31 g of **6** as a yellow solid (yield: 85%). ^{1}H NMR (400 MHz, DMSO-d_6) δ(ppm): 8.11 (d, J = 7.1 Hz, 1H, Benzothiazole, –C*H*–), 8.03 (d, J = 8.1 Hz, 1H, Benzothiazole, –C*H*–), 7.96 (s, 1H, Imidazole, –C*H*–), 7.6 (s, 1H, 5-Phenol, –C*H*–), 7.53 (t, J = 7.1 Hz, 1H, Benzothiazole, –C*H*–), 7.41 (t, J = 6.9 Hz, 1H, Benzothiazole, –C*H*–), 7.11 (s, 1H, 5-Phenol, –C*H*–), 5.48 (s, 1H, –C*H*–N), 3.24–3.18 (m, 2H, –CH_2–), 2.86–2.76 (m, 2H, –CH_2–) 2.27 (s, 3H, –CH_3). ^{13}C NMR (400 MHz, DMSO-d_6) δ(ppm): 165.74, 156.47, 151.83, 135.19, 134.94, 133.61, 128.15, 126.76, 126.50, 125.72, 125.18, 122.39, 122.28, 118.82, 54.18, 21.43, 20.72. MS (ESI): Calcd. for $C_{20}H_{18}N_4OS$ $[M+H]^+$ 363.1274, found 363.1278.

4. Supplementary Figures and Tables

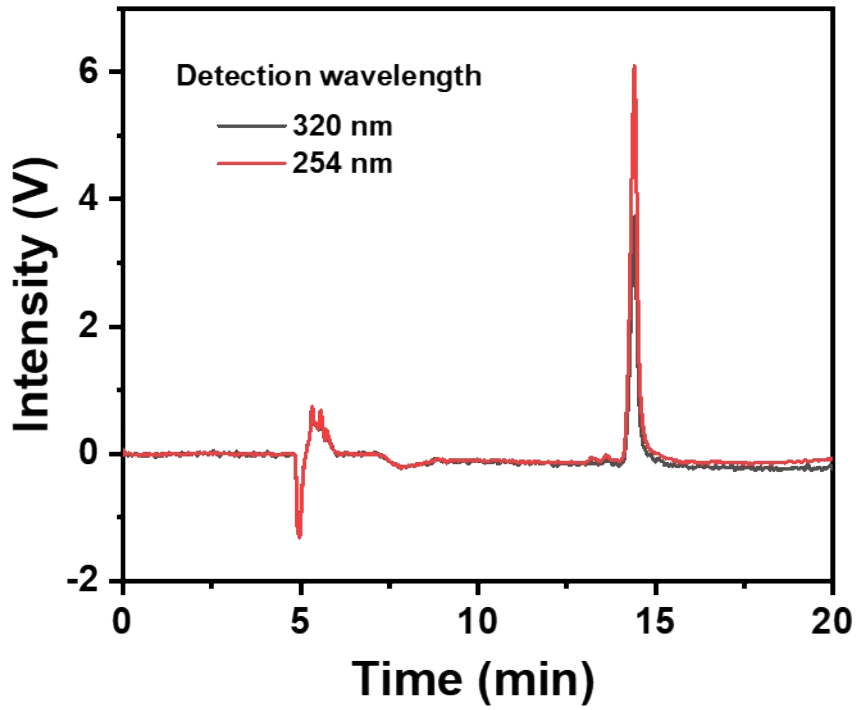

Fig. S1 High Performance Liquid Chromatogram (HPLC) of compound **2**. The mobile phase consists of methanol (containing 0.1% TEA) and water, employing a gradient elution from 10% to 90% methanol over 20 min. Detection wavelengths were set at 320 nm and 254 nm, respectively. Note: the peak at 5 min corresponds to the solvent signal.

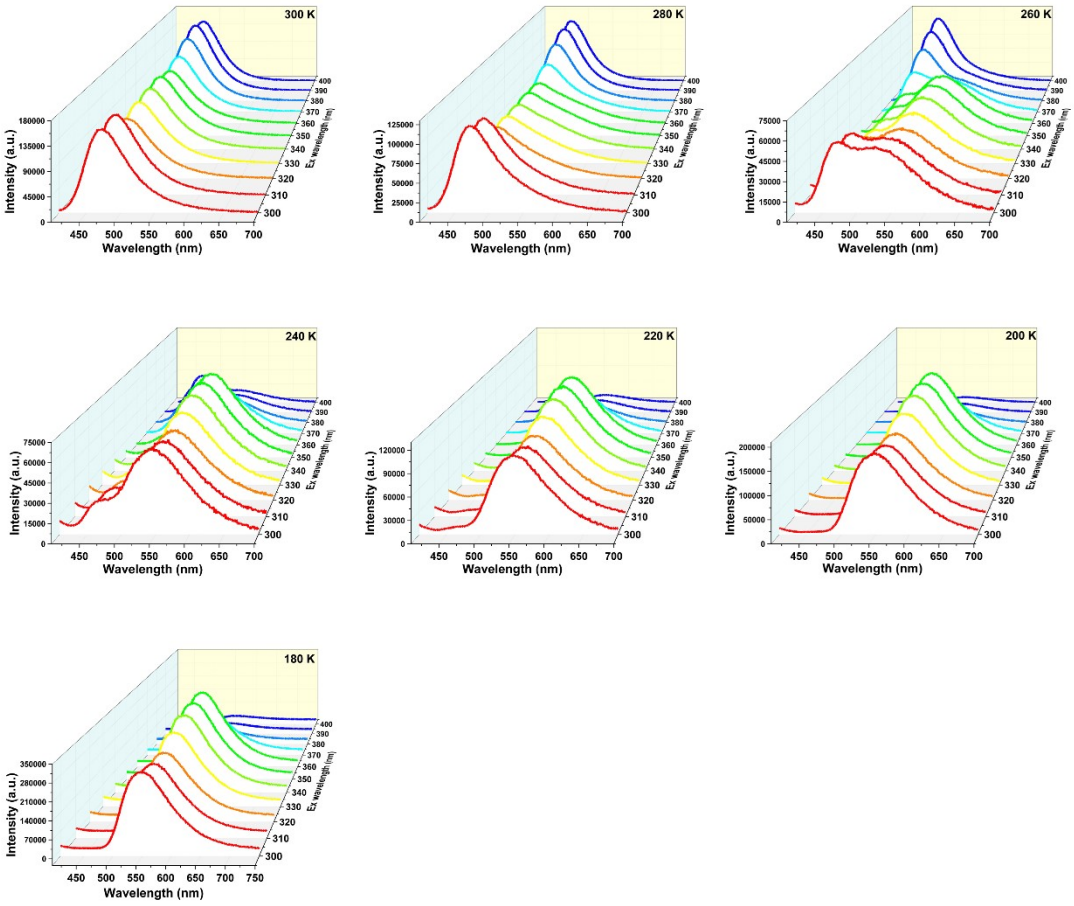

Fig. S2 PL spectra of **2** in CH_3OH with an λ_{ex} range of 300–400 nm. Concentration: 3.3×10^{-5} mol·L^{-1}, temperature range: 300 K–180 K, with test temperatures marked on the graphs.

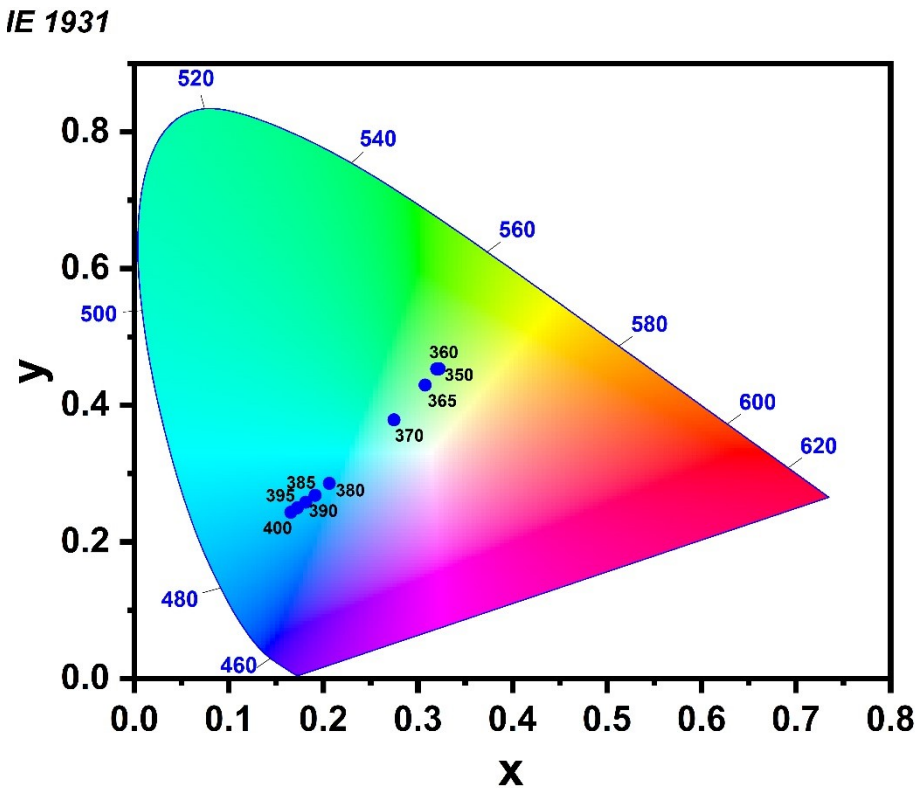

Fig. S3 Ex-De PL colors of **2** in CH_3OH, displayed in the CIE coordinate diagram.

Table S1 CIE coordinates of the Ex-De PL color of **2** in CH_3OH.

Excitation Wavelength (nm)	X	Y
350	0.31972	0.45315
360	0.32233	0.45348
365	0.30755	0.42952
370	0.27461	0.37869
380	0.2062	0.28575
385	0.19123	0.26832
390	0.18135	0.2582
395	0.17235	0.25008
400	0.16541	0.24348

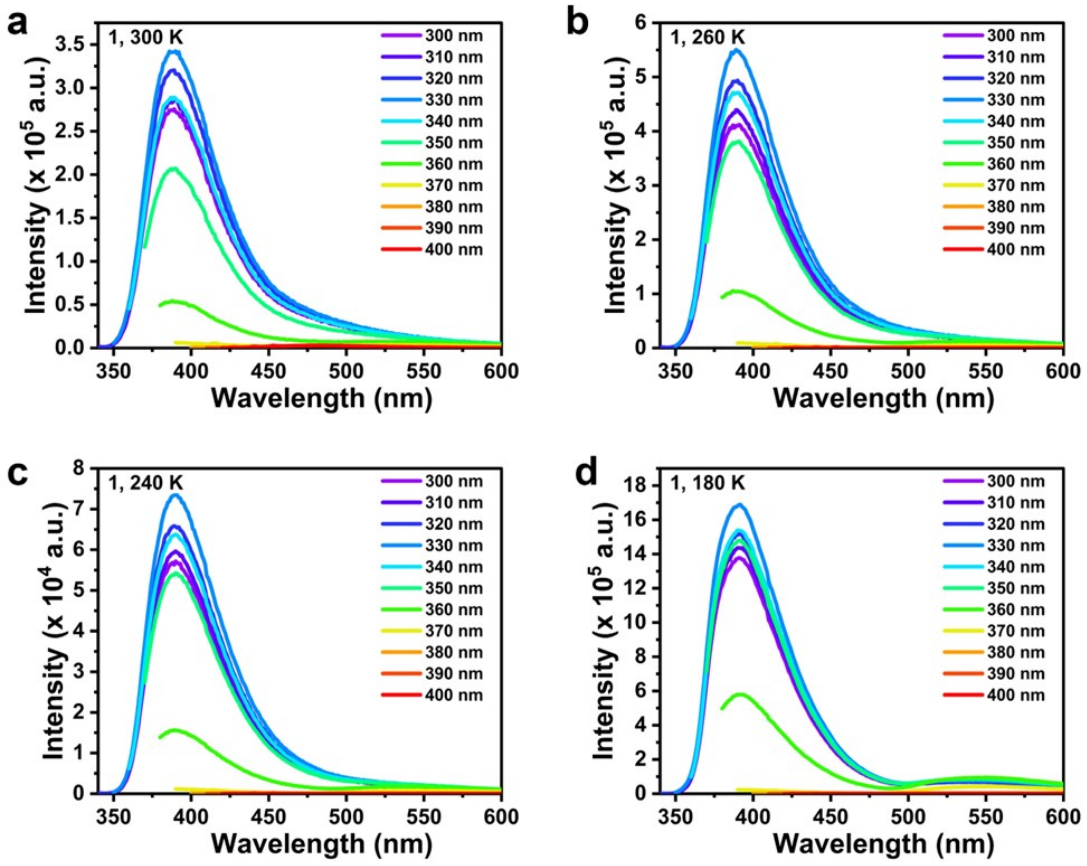

Fig. S4 PL spectra of **1** with an λ_{ex} range of 350–400 nm at (a) 300 K, (b) 260 K, (c) 240 K, and (d) 180 K with a concentration of 3.3×10^{-5} mol L^{-1} in CH_3OH. These results indicated that **1** was not an Ex-De molecule in CH_3OH.

Fig. S5 Femtosecond pump-probe transient absorption measurements system.

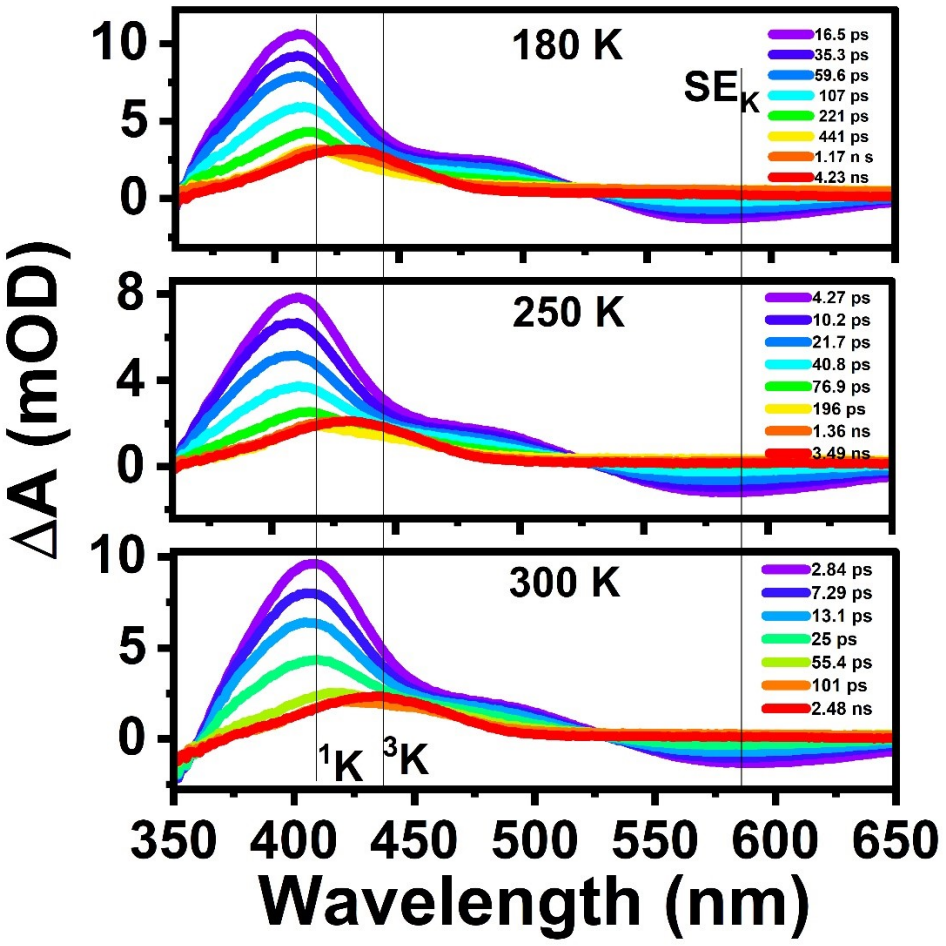

Fig. S6 fs-TA spectra of **1** under the following conditions: concentration of 3.3×10^{-4} mol· L^{-1}, λ_{ex} of 340 nm, in CH_3OH at 298 K, using a quartz cuvette with a 1 mm optical path length. Test temperatures are indicated on the graphs.

The absorption of the excited singlet state (ESA) of the keto form (K) appears at approximately 408 nm, while stimulated emission (SE) occurs around 589 nm, immediately following excitation due to the ultrafast ESIPT process. The ESA and SE features decay in dozens of picoseconds, accompanied by the formation of a new absorption feature at 430 nm, which could be reasonably attributed to the triplet state (3K*) of the Keto form due to its intrinsic ISC. These data are consistent with the findings of Aly, S. M. and co-workers.[9] The keto singlet (^{1}K), triplet (^{3}K) and keto singlet stimulated emission (SE_K) are marked in the graph.

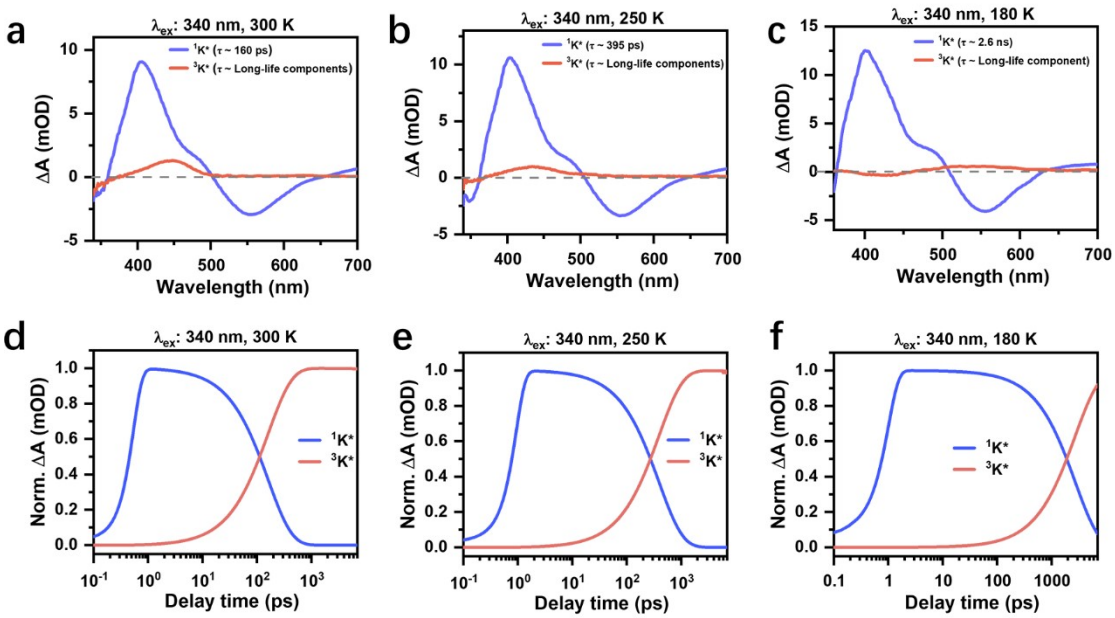

Fig. S7 Global fitting analysis of compound **2** across varying temperatures (a-f) under 340 nm excitation. (a-c) Species-associated differential spectra; (d-f) Corresponding population dynamics of transient species.

Table S2 Fitting parameters of kinetics at 408 nm under different temperature conditions.

Temperature (k)	τ (ps)
300	**163.98 ± 2.52**
250	**401.90 ± 6.53**
180	**2462.53 ± 91.05**

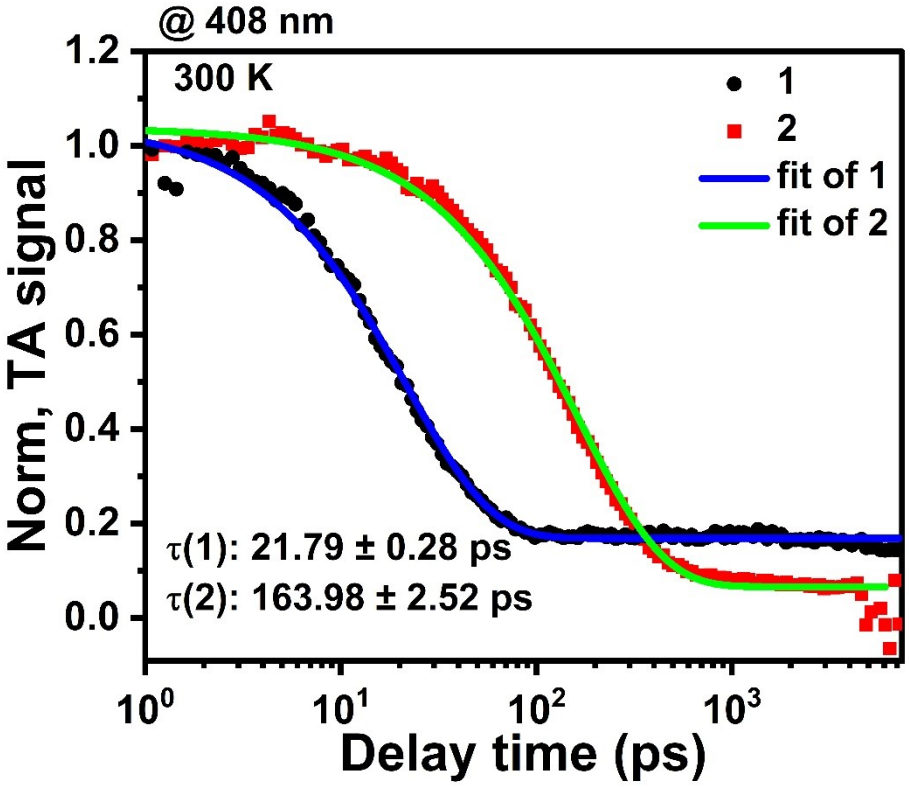

Fig. S8 fs-TA kinetic traces for **1** (black) and **2** (red) at 300 K, with solid lines showing single exponential fitting.

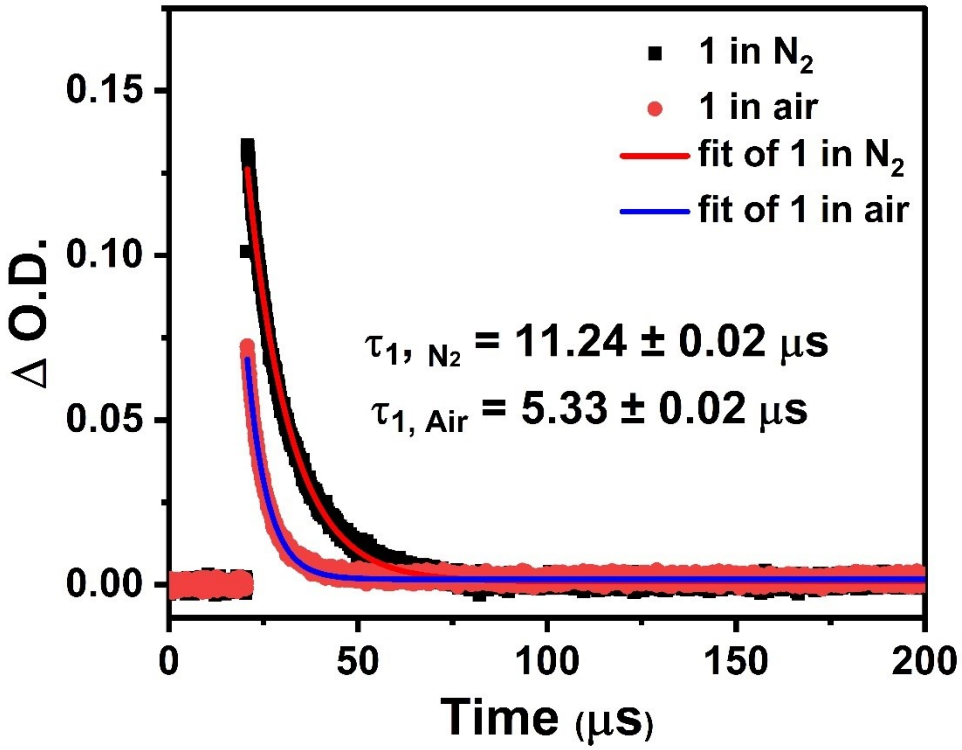

Fig. S9 Decay curve of **1** in nitrogen (N_2) and air, probed at a wavelength of 447 nm. Conditions of 33.3 μM, λ_{ex} of 355 nm, in CH_3OH, using a quartz cuvette with a 10 mm optical path length.

The ns-TA measurements demonstrated that the lifetime of the deoxygenated solution at 447 nm (11.24 μs) is significantly longer than that of the non-deoxygenated solution (5.33 μs), confirming that the 447 nm band corresponds to the keto-triplet state (^{3}K) of **1**. This longer lifetime could be attributed to the strong quenching effect of oxygen on the ^{3}K species.

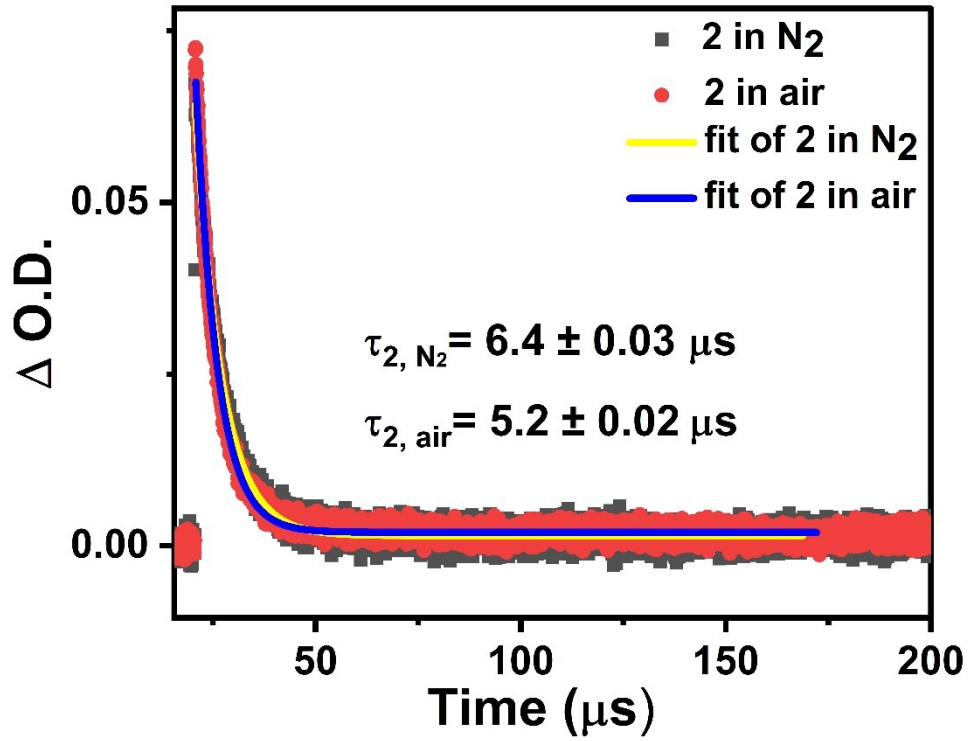

Fig. S10 Decay curve of **2** in nitrogen (N_2) and air, probed at 420 nm. Conditions: concentration of 33.3 μM, λ_{ex} of 355 nm, using a quartz cuvette with a 10 mm optical path length. The fitting method adopts single exponential fitting.

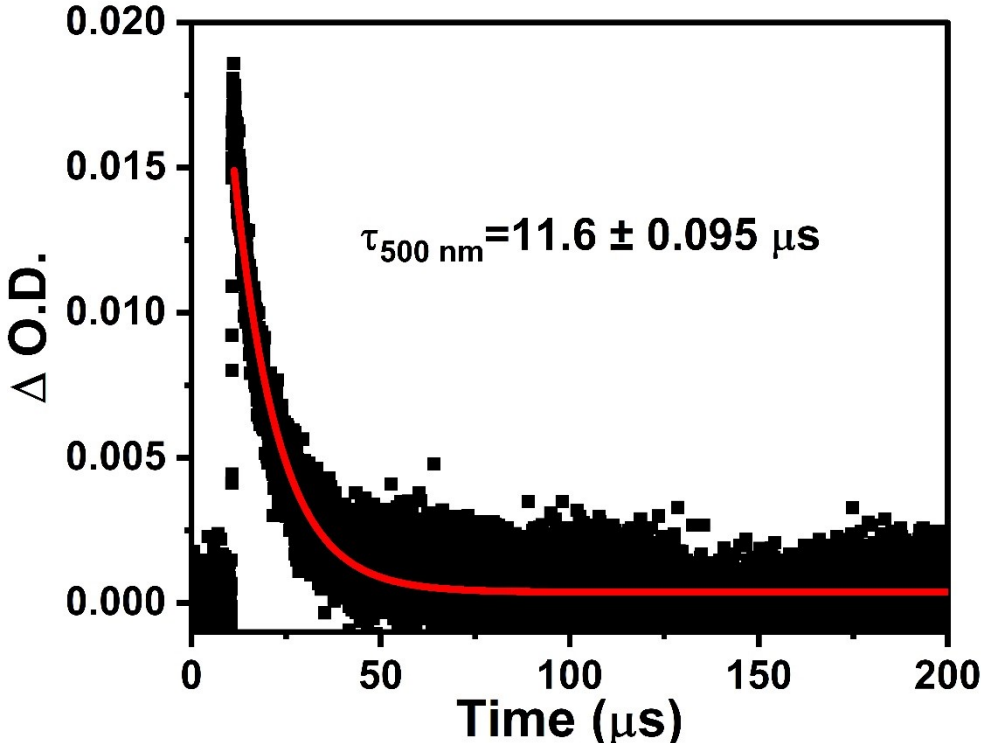

Fig. S11 Decay curve of **2** in a nitrogen atmosphere, probed at 500 nm, with a concentration of 33.3 μM and λ_{ex} of 420 nm, measured in a quartz cuvette with a 10 mm optical path length. The single exponential fitting is represented by the red line.

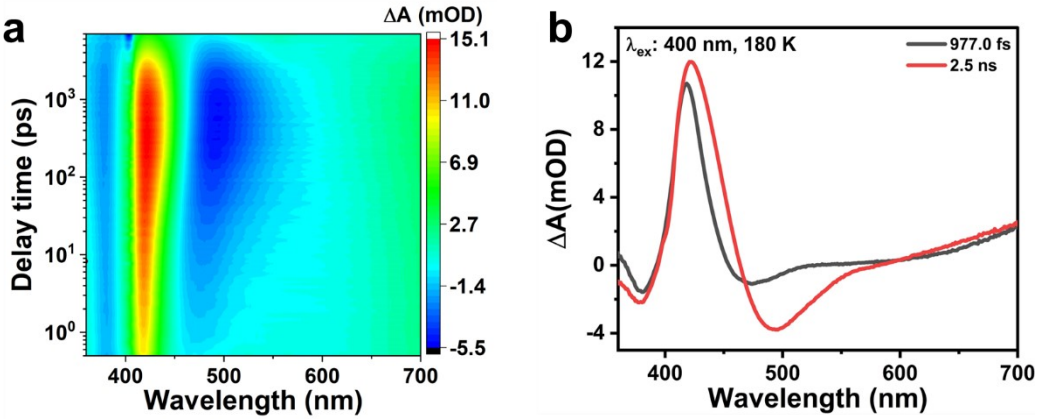

Fig. S12 fs-TA Spectra of **1** in CH_3OH at 180 K. (a) The 2D contour plots of fs-TA spectra of **2** excited by 400 nm light, and the corresponding fs-TA spectra (b) of **2** at 997 fs (black) and 2.47 ns (red).

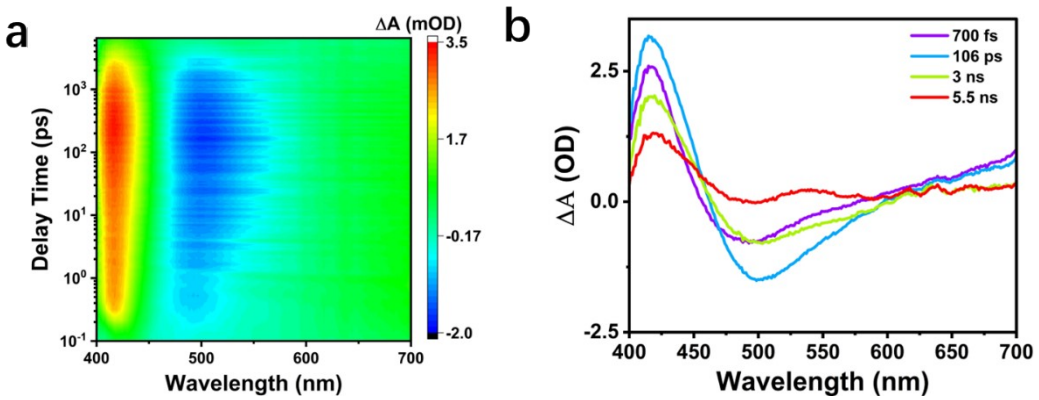

Fig. S13 fs-TA Spectra of **1** in $CH_3OH/NaOH_{(aq)}$ at 298 K. (a) The 2D contour plots of fs-TA spectra of anion of **1** excited by 400 nm light and the corresponding fs-TA spectra (b).

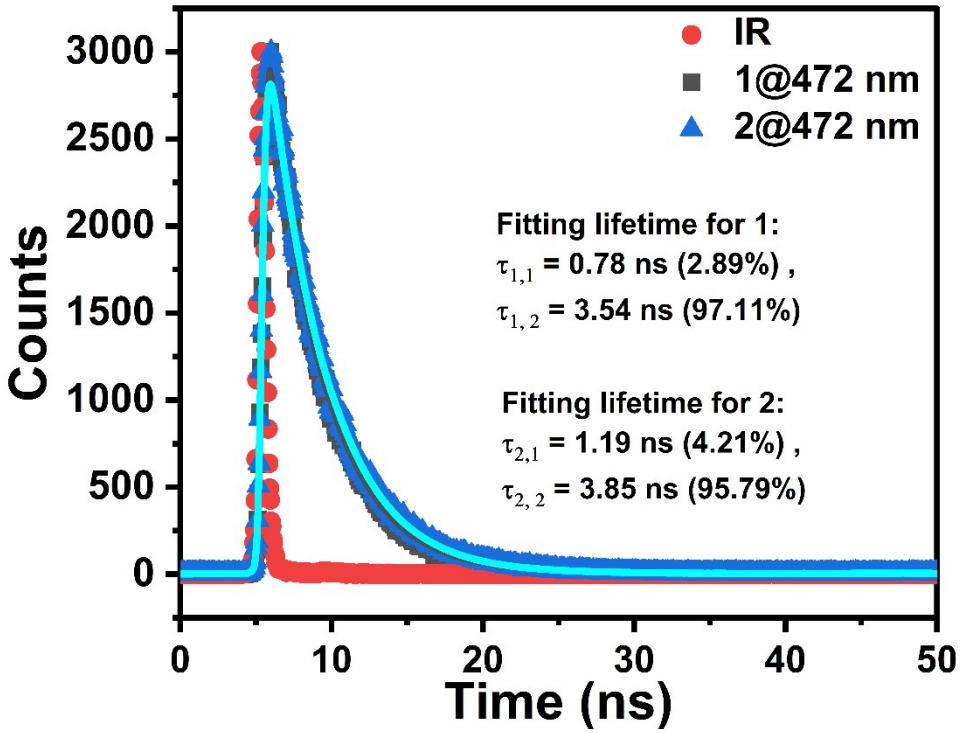

Fig. S14 Fluorescence lifetime of **2** (blue triangle) and the anion structure of **1** (black square). Compound **1** was prepared in 2 mL of 5% TEA/CH_3OH for ground state anion formation, while **2** was dissolved in pure CH_3OH, with fluorescence lifetimes measured at 472 nm.

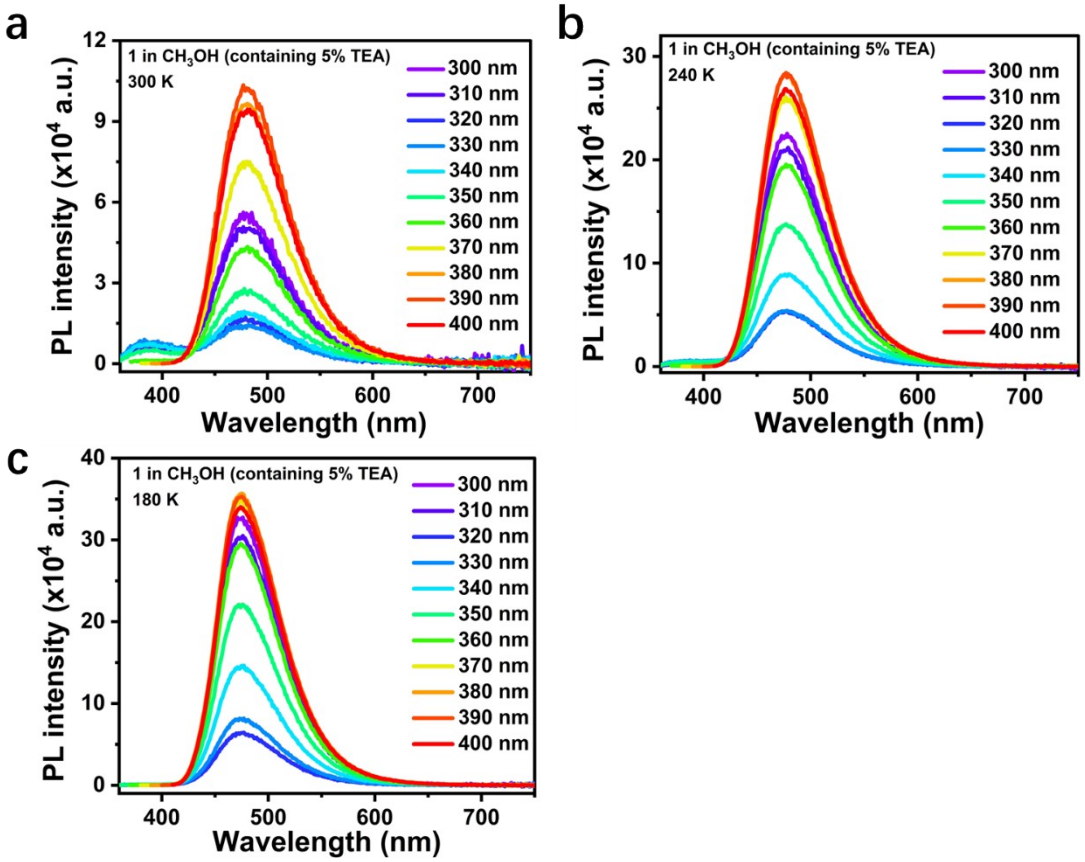

Fig. S15 PL spectra of **1** an λ_{ex} range of 350–400 nm at (a) 300 K, (b) 240 K, and (c) 180 K with a concentration of 3.3×10^{-5} mol L^{-1} in CH_3OH (containing 0.1% TEA). The results demonstrate that compound **1** does not exhibit Ex-De behavior in CH_3OH (containing 0.1% TEA).

As the temperature decreases, only the fluorescence intensity of the peak at 480 nm is found to increase, and no obvious signal of the keto-form is found.

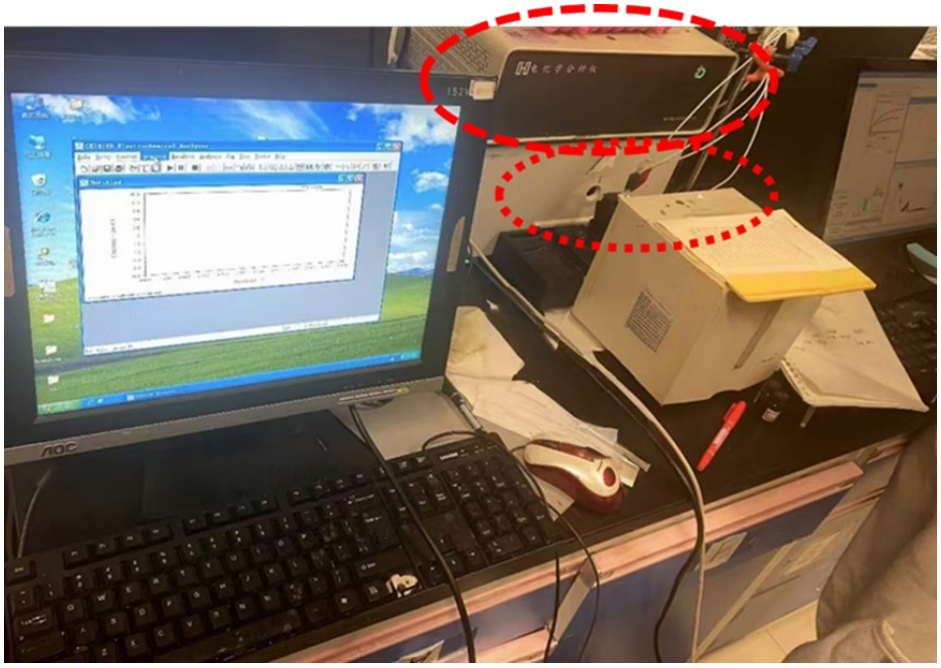

Fig. S16 Setup of the electrochemical workstation integrated with UV-visible spectroscopy for spectroelectrochemical experiments.

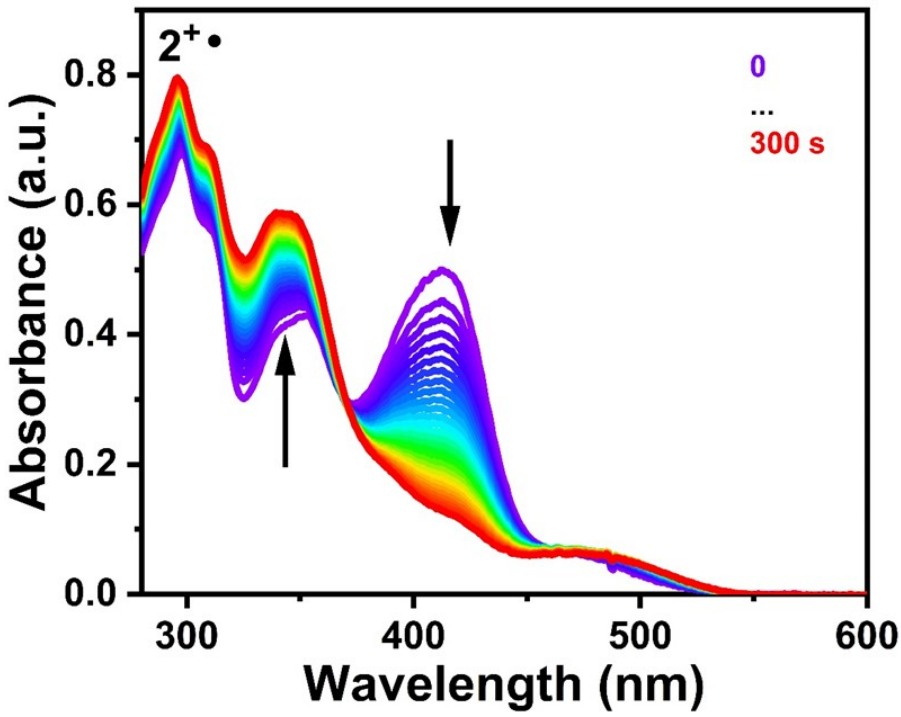

Fig. S17 Spectroelectrochemical studies of **2**: Evolution of UV-vis absorption spectra with applied oxidation potentials during oxidation at 0.27 V, with a concentration of 1.0 mM, conducted in deaerated DMSO containing 0.1 M Bu_4NPF_6 as the supporting electrode and $Ag/AgNO_3$ as the reference electrode.

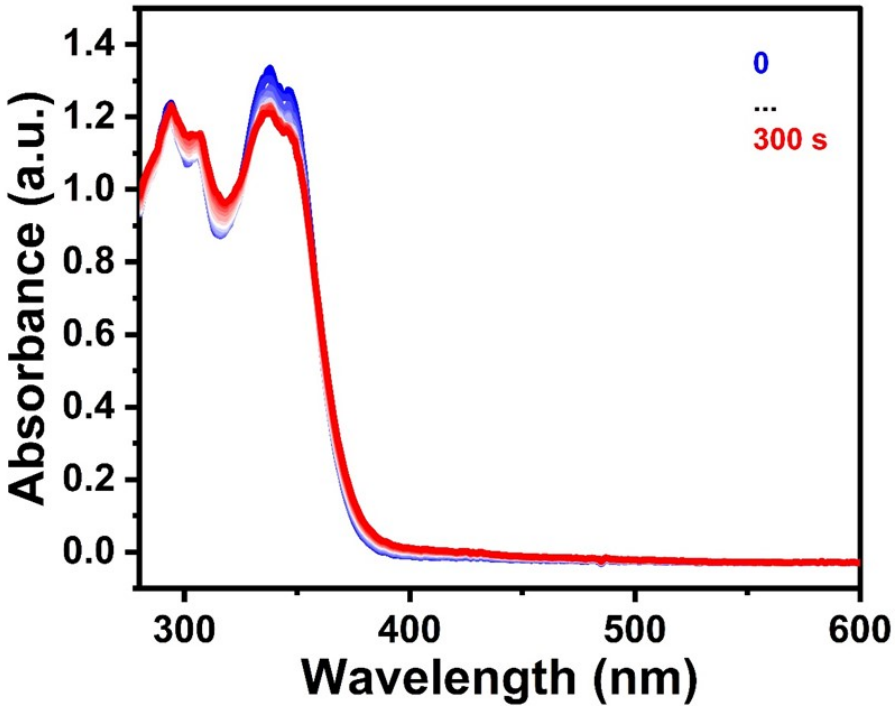

Fig. S18 Spectroelectrochemical studies of **1:** Evolution of the UV-vis absorption spectra with applied oxidation potentials during oxidation at 0.58 V, with a concentration of 1.0 mM, conducted in deaerated DMSO containing 0.1 M Bu_4NPF_6 as the supporting electrode and $Ag/AgNO_3$ as the reference electrode.

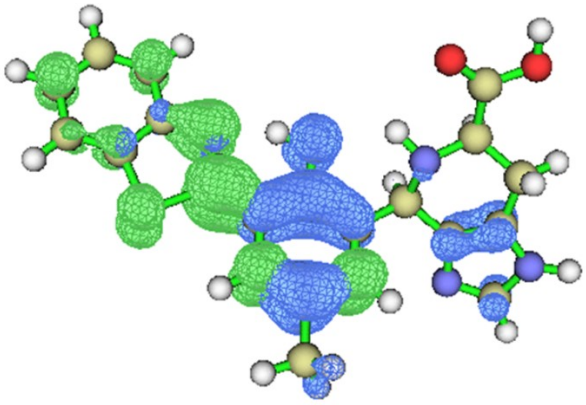

Fig. S19 Hole and electron distribution in **2**, with green and blue regions denoting the electron and hole distributions, respectively.

Table S3. Selected NTO properties for the $S_0 \rightarrow S_1$ transition

Orbital	Type	Energy (a.u.)	Energy (eV)	Occupation	Contribution
103	A+B	0.001316	0.0358	2.000000	0.13%
104	A+B	0.001534	0.0417	2.000000	0.15%
105	A+B	0.011486	0.0417	2.000000	1.15%
106	A+B	0.987853	26.8808	2.000000	98.78%
107	A+B	0.987853	26.8808	0.000000	98.78%
108	A+B	0.011486	0.3125	0.000000	1.15%
109	A+B	0.001534	0.0417	0.000000	0.15%
110	A+B	0.001316	0.0358	0.000000	0.13%

.

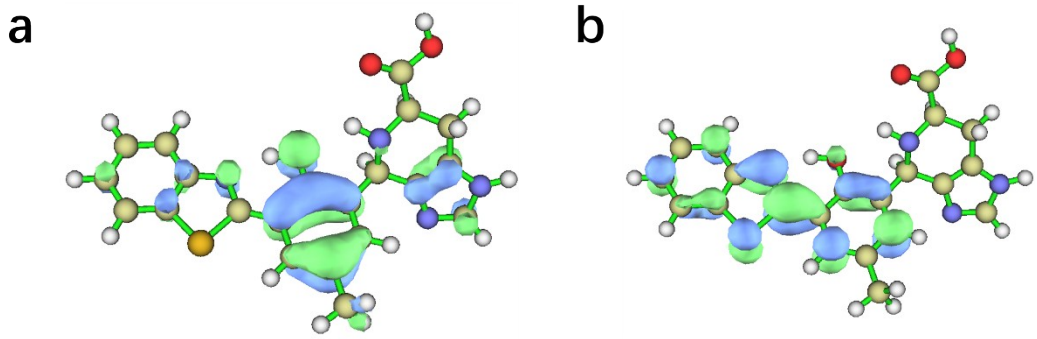

Fig. S20 Spin density surfaces of (a) NOT 106 (d) NOT107.

The natural transition orbital (NTO) analysis reveals that the electronic transition $S_0 \rightarrow S_1$ is predominantly characterized by one major NTO pair (98.79% contribution), as evidenced by the corresponding eigenvalue of 0.9879 a.u. (Table 1). This pair consists of:

- Occupied NTO (Hole orbital): Orbital 106 (E = 26.88 eV / 0.9879 a.u.)
- Unoccupied NTO (Electron Orbit): Orbital 107 (E = 26.88 eV / 0.9879 a.u.)

The degenerate energy levels (0.9879 a.u.) of these paired NTOs indicate their strong coupling in the electronic transition process. Visual representations of these orbitals generated by Multiwfn are presented in Figure S20.

Fig. S21 *In situ* Fourier transform infrared spectroscopy (FT-IR) test equipment for spectroelectrochemical experiments.

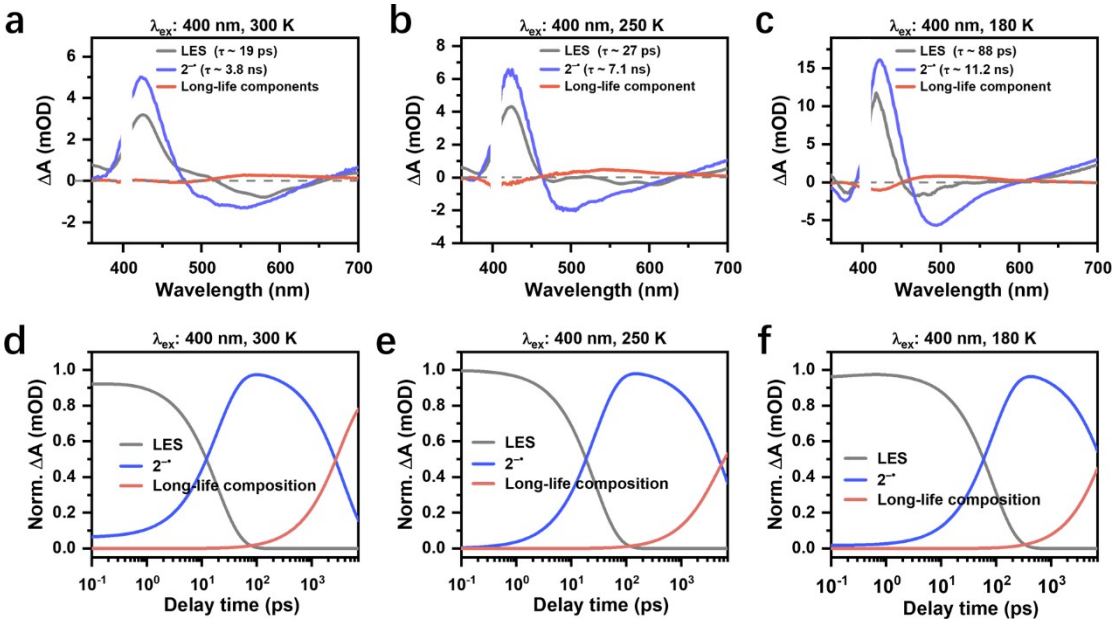

Fig. S22 Global fitting analysis of compound **2** across varying temperatures (a-f) under 400 nm excitation. (a-c) Species-associated differential spectra; (d-f) Corresponding population dynamics of transient species.

In **2**, the imidazole group in the ligand is a basic functional group. The nitrogen atom possesses lone pair electrons, which have a much stronger bonding ability with the phenolic hydroxyl group compared to methanol. As a result, the proton resides on the imidazole, while the HBT group adopts a negatively charged conformation. Upon excitation with 400 nm light, molecule **2** transforms into $\mathbf{2}^{-\bullet}$. Subsequently, through electron transfer (ET) and proton transfer (PT), the system undergoes relaxation via the PCET (Proton-Coupled Electron Transfer) process and returns to the ground state.

Compound **2** likely undergoes an E→LES→CS→PCET process following 400 nm excitation. The TA spectra primarily indicate the formation of anionic species derived from the HBT anion moiety, which are assigned as the LES species. Electrochemical spectra of **2** show that the generation of $\mathbf{2}^{-\bullet}$ is characterized by a gradual increase in the UV absorption peak at 422 nm, while the formation of $\mathbf{2}^{+\bullet}$ is evidenced by enhanced absorption in the 280-360 nm range. Consequently, the spectral changes observed in the visible region of the TA spectra correspond to the $\mathbf{2}^{-\bullet}$ species.

The fs-TA spectra were globally fitted using Glotaran software with a sequential model.[10] The excited-state evolution pathway LES→$\mathbf{2}^{-\bullet}$→long-lived component was employed to analyze the 400 nm excitation spectrum, which revealed the dynamics of three distinct components as demonstrated in Fig. S22.

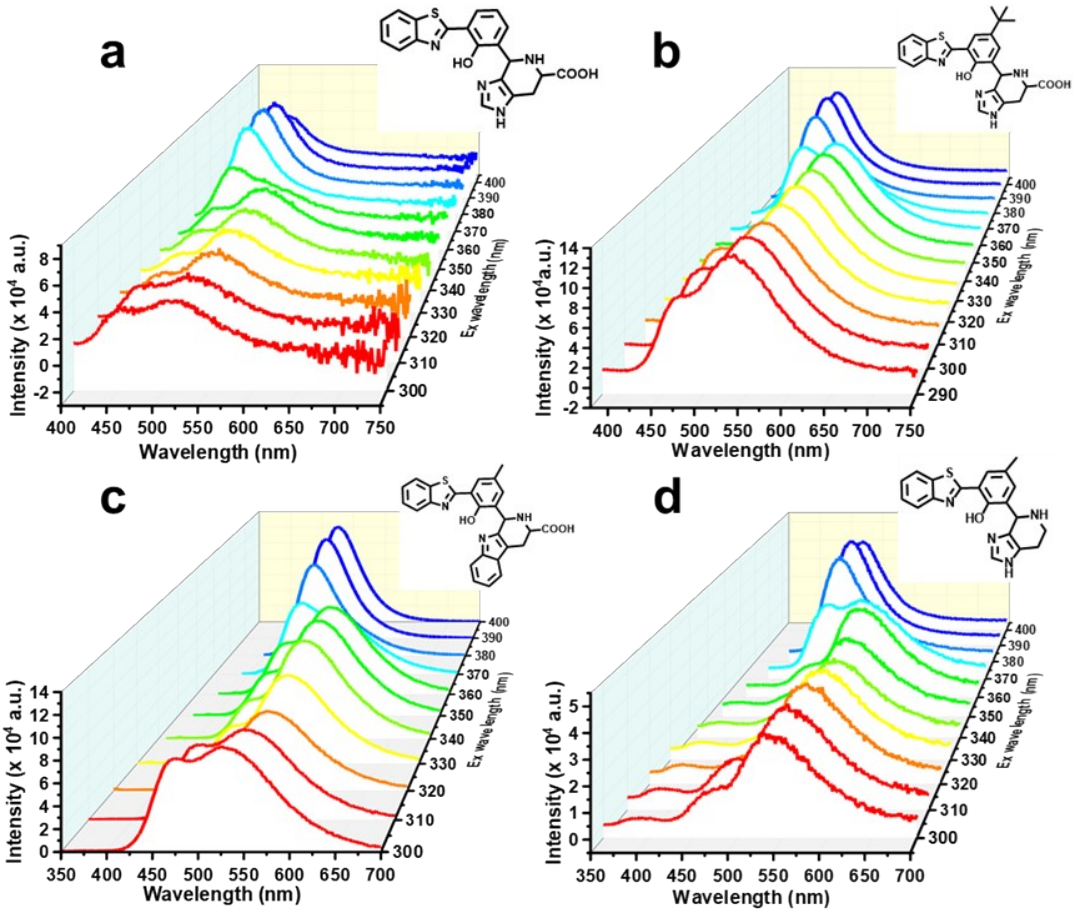

Fig. S23 Ex-De PL spectra of molecules (a) **3** (temperature: 260 K), (b) **4** (temperature: 260 K), (c) **5** (temperature: 260 K), and (d) **6** (temperature: 220 K). The concentrations are 5.0×10^{-5} mol· L^{-1} in CH_3OH. The inset in the upper right corner of each spectrum displays the corresponding molecular structure. **3**, **4**, **5**, and **6** share the same structure framework as **2**, featuring an HBT luminophore and a nitrogen-containing imidazole structure, and exhibit excitation wavelength-dependent PL in CH_3OH solutions.

Table S4 CIE coordinates of the Ex-De PL color of compound **3**, **4**, **5** and **6** in CH_3OH.

Excitation Wavelength (nm)	3		4		5		6	
	X	Y	X	Y	X	Y	X	Y
300	0.2224	0.3421	0.2969	0.4276	0.2859	0.4176	0.3308	0.4861
310	0.2261	0.3398	0.2918	0.4201	0.2914	0.4124	0.3260	0.4834
320	0.2410	0.3914	0.3164	0.4612	0.3145	0.4569	0.3530	0.5235
330	0.2493	0.4027	0.3276	0.4789	0.3323	0.4799	0.3555	0.5294
340	0.2412	0.3946	0.3345	0.4879	0.3362	0.4840	0.3552	0.5319
350	0.2401	0.3879	0.3348	0.4868	0.3302	0.4750	0.3507	0.5235
360	0.1976	0.2504	0.3229	0.4635	0.3171	0.4566	0.3440	0.5118
370	0.1611	0.1478	0.2477	0.3428	0.2541	0.3725	0.2752	0.4079
380	0.1557	0.1310	0.1902	0.2576	0.1834	0.2818	0.1834	0.2784
390	0.1537	0.1273	0.1722	0.2377	0.1577	0.2543	0.1621	0.2505
400	0.1455	0.1264	0.1634	0.2328	0.1497	0.2488	0.1559	0.2451

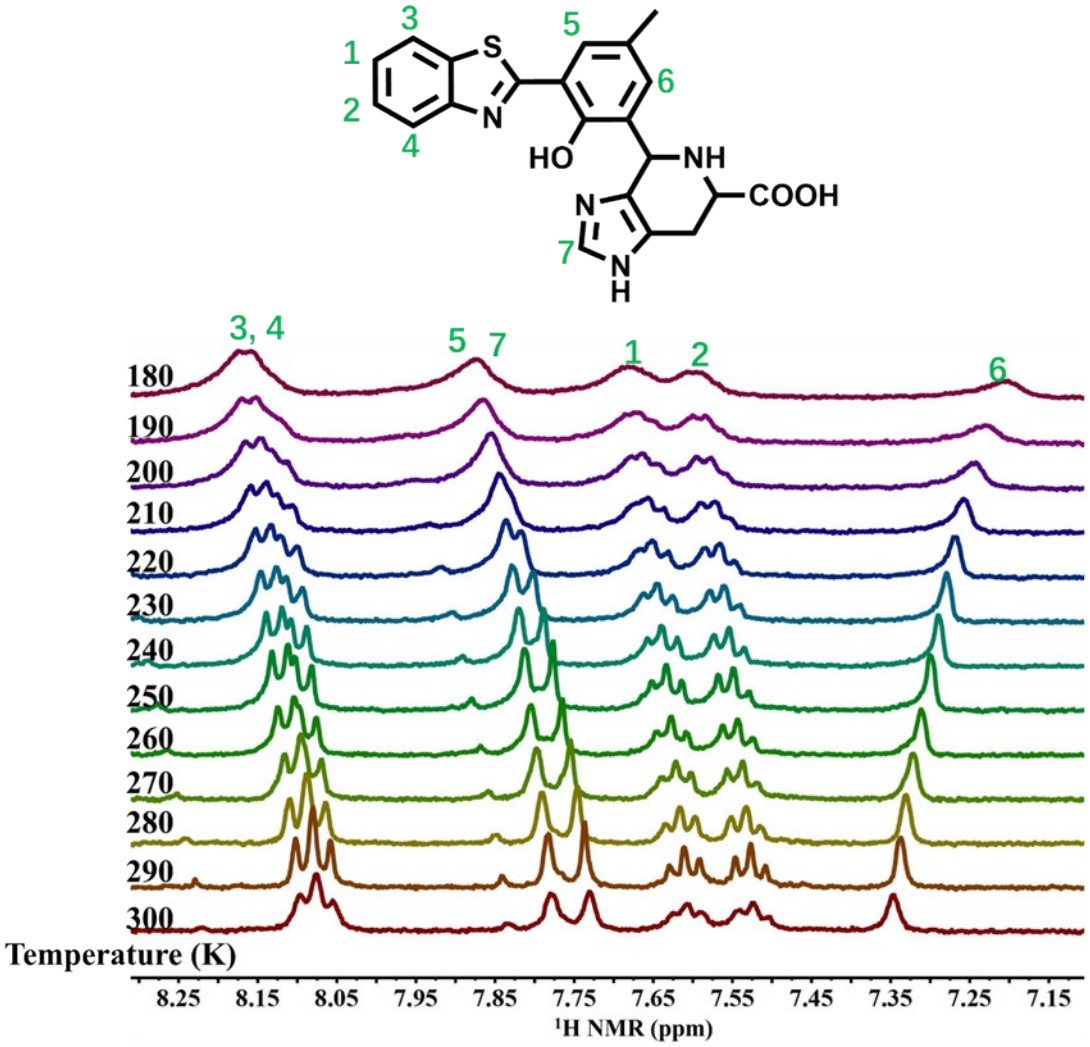

Fig. S24 ^{1}H NMR spectra of **2** at different temperatures in CD_3OD. When the temperature decreases from 300 K to 180 K, H6 peak displays a high-field shift, while H5 and H7 peaks shift to lower fields, ultimately merging into one peak. Additionally, H3 and H4 show down-field shifts and splitting behaviors.

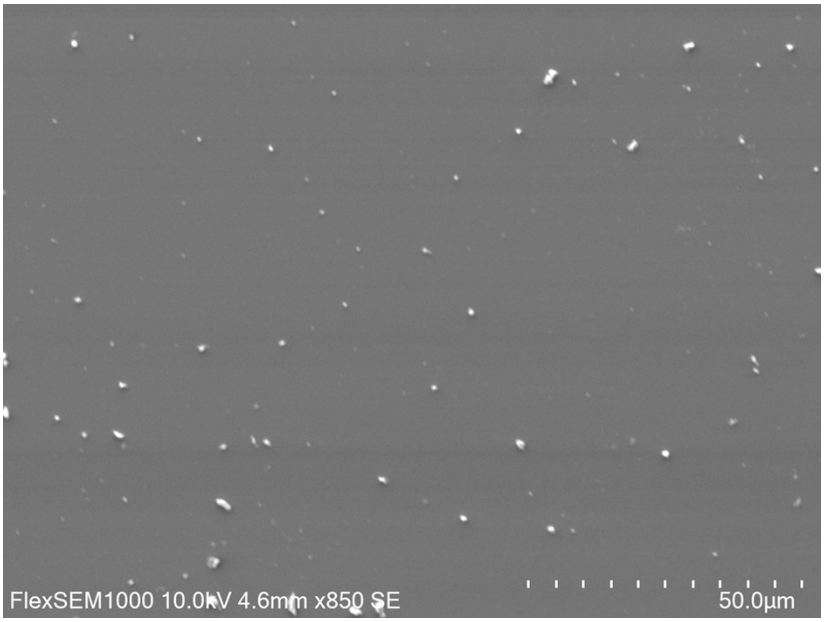

Fig. S25 SEM images of compound 2 in CH_3OH, concentrations: 0.33 mM. The samples were prepared by dropping one droplet of solution on the silica wafer surfaces, allowing them to dry naturally.

Compound **2** was prepared at the highest concentration used in all spectroscopic measurements for SEM imaging, with no observable aggregate formation. This confirms that the spectral features obtained in our experiments are not caused by molecular aggregation.

Cartesian Coordinates

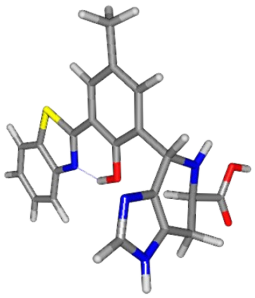

Enol-form

$^{E}S_0$-Min

Atom	X	Y	Z
C	-3.542111000	-1.272766000	0.051024000
C	-4.576754000	-0.326768000	-0.139528000
C	-5.914108000	-0.716741000	-0.214984000
C	-6.206898000	-2.074163000	-0.096502000
C	-5.186751000	-3.022336000	0.092965000
C	-3.853893000	-2.633776000	0.167943000
C	-2.271032000	0.575753000	-0.033300000
H	-6.703580000	0.012805000	-0.361209000
H	-7.240427000	-2.401544000	-0.151716000
H	-5.443808000	-4.073212000	0.182041000
H	-3.057986000	-3.356722000	0.314071000
S	-3.890155000	1.284684000	-0.249285000
N	-2.271585000	-0.728313000	0.104029000
C	-1.061983000	1.383846000	-0.011380000
C	0.200659000	0.760692000	0.179072000
C	-1.125482000	2.781756000	-0.177064000
C	1.370586000	1.552631000	0.213294000
C	0.011139000	3.573125000	-0.152713000
H	-2.093387000	3.252640000	-0.327710000
C	1.244177000	2.928658000	0.049271000
H	2.148383000	3.533279000	0.083230000
C	2.777560000	0.978194000	0.396921000
C	2.921214000	-0.004628000	1.518309000
C	3.355763000	-1.290299000	1.334484000
C	3.053168000	-1.044251000	-1.061685000
C	2.936369000	-0.888659000	3.469418000
H	2.854159000	-1.072625000	4.531562000
N	2.659487000	0.246856000	2.850844000
N	3.362593000	-1.850683000	2.595220000
H	3.627828000	-2.797158000	2.831479000

C	3.540445000	-1.454687000	-2.438553000
O	3.249201000	-0.523498000	-3.372322000
H	3.567266000	-0.861311000	-4.231631000
O	4.085317000	-2.505526000	-2.706802000
C	3.689256000	-1.924396000	0.028524000
H	4.773286000	-1.985787000	-0.130477000
H	3.294005000	-2.942828000	-0.046527000
N	3.371110000	0.374359000	-0.821943000
H	3.080296000	0.918847000	-1.629226000
O	0.315556000	-0.573674000	0.332957000
H	-0.600686000	-0.968849000	0.288672000
C	-0.057569000	5.069745000	-0.330311000
H	0.368834000	5.593348000	0.533690000
H	0.507865000	5.392826000	-1.212782000
H	-1.091082000	5.407252000	-0.451837000
H	3.409005000	1.847129000	0.625003000
H	1.968147000	-1.232550000	-1.057020000

$^{E}S_1$-Min

Atom	X	Y	Z
C	-3.438749000	-1.226392000	0.216127000
C	-4.513982000	-0.312996000	-0.006011000
C	-5.839102000	-0.725427000	-0.013596000
C	-6.124906000	-2.082379000	0.201320000
C	-5.081848000	-2.994430000	0.419458000
C	-3.750610000	-2.586771000	0.429915000
C	-2.209162000	0.660541000	-0.033602000
H	-6.641385000	-0.013304000	-0.183577000
H	-7.155929000	-2.422074000	0.197206000
H	-5.315480000	-4.043045000	0.584497000
H	-2.946088000	-3.296126000	0.599688000
S	-3.869586000	1.319094000	-0.248997000
N	-2.195308000	-0.677694000	0.200787000
C	-1.034601000	1.460168000	-0.088443000
C	0.260381000	0.844492000	0.100937000
C	-1.048539000	2.847726000	-0.331551000
C	1.425701000	1.612431000	0.010474000
C	0.120379000	3.621977000	-0.421996000
H	-2.007861000	3.344397000	-0.458072000
C	1.354626000	2.992766000	-0.281969000
H	2.272961000	3.566442000	-0.362877000
C	2.805087000	0.981115000	0.170418000
C	3.050125000	0.162715000	1.398252000

C	3.382473000	-1.165465000	1.366641000
C	2.801396000	-1.287054000	-1.006912000
C	3.278467000	-0.414306000	3.442210000
H	3.329254000	-0.428033000	4.521552000
N	2.984485000	0.633087000	2.690093000
N	3.526137000	-1.527253000	2.688051000
H	3.765066000	-2.445665000	3.037648000
C	3.112724000	-1.913051000	-2.357057000
O	3.047669000	-1.017107000	-3.355775000
H	3.231649000	-1.476687000	-4.197893000
O	3.350104000	-3.089654000	-2.501285000
C	3.519135000	-2.016106000	0.152736000
H	4.568831000	-2.185205000	-0.115236000
H	3.054553000	-2.997395000	0.276425000
N	3.053782000	0.131361000	-1.000178000
H	3.035775000	0.596706000	-1.902730000
O	0.345823000	-0.479904000	0.366134000
H	-0.610345000	-0.849887000	0.361644000
C	0.025144000	5.110283000	-0.645071000
H	-0.295595000	5.630137000	0.267166000
H	0.990299000	5.530162000	-0.944138000
H	-0.708928000	5.348881000	-1.423482000
H	3.538827000	1.792210000	0.103902000
H	1.710488000	-1.399228000	-0.835297000

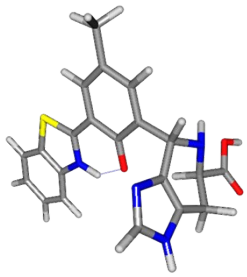

Keto-form

$^{K}S_0$-Min

Atom	X	Y	Z
C	-3.489114000	-1.279584000	0.137408000
C	-4.536935000	-0.359330000	-0.051436000
C	-5.865586000	-0.776790000	-0.063294000
C	-6.126827000	-2.135349000	0.118507000
C	-5.082264000	-3.052778000	0.307159000
C	-3.752426000	-2.638623000	0.319115000
C	-2.252476000	0.669427000	-0.075731000
H	-6.673071000	-0.067517000	-0.208992000
H	-7.154413000	-2.483977000	0.113471000

H	-5.311458000	-4.104288000	0.446490000
H	-2.939787000	-3.342370000	0.464551000
S	-3.896084000	1.275742000	-0.250755000
N	-2.251218000	-0.659597000	0.113694000
C	-1.066927000	1.437782000	-0.119051000
C	0.206561000	0.750206000	0.059105000
C	-1.120647000	2.842472000	-0.334225000
C	1.388936000	1.587281000	0.030177000
C	0.017790000	3.608071000	-0.371580000
H	-2.089348000	3.318190000	-0.474091000
C	1.261549000	2.942408000	-0.177575000
H	2.167664000	3.547227000	-0.190062000
C	2.787645000	1.006047000	0.218113000
C	2.955017000	0.166171000	1.448546000
C	3.383512000	-1.134323000	1.417969000
C	2.986613000	-1.196659000	-0.971288000
C	3.030675000	-0.462772000	3.496361000
H	2.980216000	-0.509674000	4.575309000
N	2.736052000	0.586058000	2.746413000
N	3.428801000	-1.530347000	2.739379000
H	3.700531000	-2.440422000	3.085535000
C	3.394590000	-1.792944000	-2.302367000
O	3.065059000	-0.989493000	-3.337988000
H	3.330477000	-1.448474000	-4.158041000
O	3.910335000	-2.881373000	-2.458486000
C	3.674447000	-1.929831000	0.192872000
H	4.752472000	-2.007813000	0.001322000
H	3.284484000	-2.950738000	0.263577000
N	3.319584000	0.239574000	-0.938560000
H	2.981552000	0.673303000	-1.793193000
O	0.275976000	-0.513571000	0.235816000
H	-1.287188000	-1.056441000	0.222889000
C	-0.016679000	5.097747000	-0.601082000
H	0.439788000	5.642844000	0.234811000
H	0.539518000	5.377681000	-1.504812000
H	-1.043973000	5.457167000	-0.715067000
H	3.449767000	1.877740000	0.314830000
H	1.901888000	-1.360384000	-0.873897000

$^{K}S_1$-Min

Atom	X	Y	Z
C	-3.504758000	-1.172800000	0.388304000

C	-4.495325000	-0.263509000	-0.056154000
C	-5.822128000	-0.653426000	-0.189480000
C	-6.161761000	-1.975593000	0.123921000
C	-5.182349000	-2.879556000	0.559953000
C	-3.850086000	-2.497416000	0.698845000
C	-2.187792000	0.721332000	0.078422000
H	-6.575730000	0.047969000	-0.532229000
H	-7.192668000	-2.299727000	0.025902000
H	-5.465056000	-3.901047000	0.795847000
H	-3.092417000	-3.196452000	1.036980000
S	-3.778428000	1.322589000	-0.388360000
N	-2.270230000	-0.587962000	0.468972000
C	-0.963204000	1.474037000	0.030951000
C	0.320440000	0.783408000	0.206124000
C	-0.973615000	2.847696000	-0.158246000
C	1.511195000	1.574315000	0.104834000
C	0.220966000	3.619296000	-0.273819000
H	-1.925421000	3.372195000	-0.214894000
C	1.433367000	2.962323000	-0.151946000
H	2.358078000	3.528829000	-0.233626000
C	2.887398000	0.942151000	0.164611000
C	3.152150000	0.055678000	1.342298000
C	3.436480000	-1.281042000	1.227956000
C	2.728692000	-1.223373000	-1.094430000
C	3.450083000	-0.640648000	3.345231000
H	3.552089000	-0.714721000	4.418857000
N	3.160747000	0.454842000	2.663073000
N	3.625770000	-1.718880000	2.521411000
H	3.850714000	-2.661102000	2.810813000
C	2.880290000	-1.818345000	-2.478835000
O	2.606973000	-0.921142000	-3.449290000
H	2.690366000	-1.380469000	-4.307033000
O	3.159305000	-2.976763000	-2.708523000
C	3.459597000	-2.069233000	-0.035102000
H	4.483884000	-2.279219000	-0.368565000
H	2.951225000	-3.032724000	0.073059000
N	3.200461000	0.160051000	-1.062599000
H	2.884328000	0.663977000	-1.886835000
O	0.350259000	-0.480308000	0.438492000
H	-1.362115000	-1.042684000	0.639779000
C	0.128360000	5.099538000	-0.507868000
H	-0.414077000	5.597611000	0.307017000
H	1.119869000	5.554105000	-0.584996000

H	-0.423568000	5.321783000	-1.431121000
H	3.610338000	1.767199000	0.180385000
H	1.647477000	-1.266592000	-0.850430000

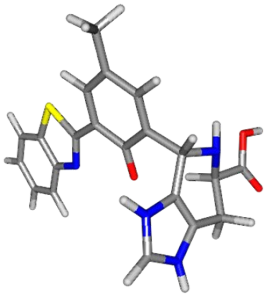

The proton transferred from HBT to the imidazole group

S_0-Min

Atom	X	Y	Z
C	3.675668000	-1.261093000	-0.213311000
C	4.622183000	-0.305412000	0.237633000
C	5.967140000	-0.633649000	0.405712000
C	6.371999000	-1.939104000	0.121787000
C	5.446884000	-2.895997000	-0.324715000
C	4.104684000	-2.567034000	-0.494527000
C	2.242681000	0.450507000	-0.029219000
H	6.683985000	0.105420000	0.749873000
H	7.414910000	-2.214146000	0.248620000
H	5.782790000	-3.906084000	-0.540860000
H	3.382811000	-3.300470000	-0.840758000
S	3.814228000	1.223140000	0.511894000
N	2.377195000	-0.808672000	-0.346672000
C	1.038576000	1.252852000	-0.046555000
C	-0.274034000	0.629219000	-0.186487000
C	1.144412000	2.655034000	0.102036000
C	-1.396892000	1.557649000	-0.170303000
C	0.056212000	3.509570000	0.113498000
H	2.135526000	3.096145000	0.192002000
C	-1.218452000	2.920426000	-0.032408000
H	-2.096107000	3.567769000	-0.039033000
C	-2.816561000	1.026360000	-0.296581000
C	-2.993694000	0.047841000	-1.411158000
C	-3.465903000	-1.225134000	-1.288173000
C	-3.095192000	-1.039085000	1.095243000
C	-2.976738000	-0.876107000	-3.434549000
H	-2.854355000	-1.019375000	-4.494987000
N	-2.703958000	0.239566000	-2.746150000

N	-3.443636000	-1.774047000	-2.559213000
H	-3.723617000	-2.715974000	-2.806357000
C	-3.515821000	-1.499336000	2.473773000
O	-3.201243000	-0.594418000	3.424293000
H	-3.470329000	-0.968283000	4.285414000
O	-4.029753000	-2.569962000	2.726891000
C	-3.800127000	-1.874335000	0.009269000
H	-4.882202000	-1.890571000	0.182002000
H	-3.442324000	-2.907114000	0.041651000
N	-3.410087000	0.391393000	0.911712000
H	-3.072611000	0.905228000	1.721274000
O	-0.463414000	-0.616949000	-0.311042000
H	-2.310973000	1.081849000	-3.149695000
C	0.209892000	5.004101000	0.258406000
H	-0.193358000	5.544048000	-0.608868000
H	-0.319715000	5.385878000	1.141483000
H	1.263831000	5.283614000	0.359711000
H	-3.455872000	1.893796000	-0.509482000
H	-2.012841000	-1.222666000	1.002607000

S_1-Min

Atom	X	Y	Z
C	-3.713301000	-1.157842000	0.265853000
C	-4.542188000	-0.234988000	-0.457473000
C	-5.837936000	-0.552765000	-0.842290000
C	-6.351978000	-1.817509000	-0.510084000
C	-5.556950000	-2.737843000	0.196076000
C	-4.259403000	-2.429126000	0.584560000
C	-2.218311000	0.501805000	0.126965000
H	-6.446320000	0.161441000	-1.390328000
H	-7.365164000	-2.080283000	-0.799057000
H	-5.966470000	-3.714642000	0.442647000
H	-3.647444000	-3.145727000	1.124915000
S	-3.644687000	1.257708000	-0.721565000
N	-2.470441000	-0.725504000	0.593236000
C	-1.020423000	1.289913000	0.306970000
C	0.294818000	0.627400000	0.389581000
C	-1.066549000	2.680509000	0.369529000
C	1.454862000	1.461643000	0.562311000
C	0.101628000	3.487698000	0.466187000
H	-2.032799000	3.178812000	0.355321000
C	1.341142000	2.864547000	0.572641000

H	2.239801000	3.470794000	0.664606000
C	2.846377000	0.861516000	0.590901000
C	2.970283000	-0.366894000	1.431747000
C	3.350982000	-1.597668000	0.986117000
C	3.018418000	-0.794851000	-1.275643000
C	2.902724000	-1.760763000	3.162764000
H	2.779239000	-2.154480000	4.157723000
N	2.701521000	-0.494401000	2.779373000
N	3.300723000	-2.442383000	2.082085000
H	3.518548000	-3.432062000	2.082464000
C	3.437854000	-0.915475000	-2.728056000
O	3.167741000	0.210742000	-3.418130000
H	3.438641000	0.063358000	-4.344825000
O	3.918788000	-1.907126000	-3.234714000
C	3.638095000	-1.928219000	-0.436634000
H	4.716017000	-1.990959000	-0.622365000
H	3.195416000	-2.887357000	-0.719137000
N	3.431414000	0.511298000	-0.736421000
H	3.165521000	1.240203000	-1.393784000
O	0.393600000	-0.635393000	0.283330000
H	2.374151000	0.244138000	3.391196000
C	-0.030380000	4.983642000	0.466858000
H	0.937429000	5.474390000	0.603490000
H	-0.465142000	5.341938000	-0.476476000
H	-0.703973000	5.321343000	1.265924000
H	3.512188000	1.628615000	1.006449000
H	1.923215000	-0.920080000	-1.248812000

5. Reference

1. M. Liu, P. Xia, G. Zhao, C. Nie, K. Gao, S. He, L. Wang and K. Wu, *Angew. Chem. Int. Ed.*, 2022, **61**, e202208241.
2. C. Yang, F. Artizzu, K. Folens, G. Du Laing and R. Van Deun, *J. Mater. Chem. C*, 2021, **9**, 7154-7162.
3. X. Xiao, Y. Yan, A. A. Sukhanov, S. Doria, A. Iagatti, L. Bussotti, J. Zhao, M. Di Donato and V. K. Voronkova, *J. Phys. Chem. B*, 2023, **127**, 6982-6998.
4. Y. Wu, Z. Zhao and Z. Peng, *ACS Energy Letters*, 2023, **8**, 3430-3436.
5. M. J. Frisch, *et al.* Gaussian 16, Revision C.01(Gaussian, Inc., Wallingford CT, 2016)
6. Z. Huang, S. Ding, D. Yu, F. Huang and G. Feng, *Chem. Commun.*, 2014, **50**, 9185-9187.
7. W. Xu, G. Han, P. Ma, Q. Diao, L. Xu, X. Liu, Y. Sun, X. Wang and D. Song, *Sens. Actuators B: Chemical*, 2017, **251**, 366-373.
8. N. N. Smolyar, M. G. Abramyants, T. I. Zavyazkina, D. I. Matveeva, Y. S. Borodkin and I. A. Voloskii, *Russ. J. Org. Chem.*, 2009, **45**, 1219-1223.
9. S. M. Aly, A. Usman, M. AlZayer, G. A. Hamdi, E. Alarousu and O. F. Mohammed, *J. Phys. Chem. B*, 2015, **119**, 2596-2603.
10. J. J. Snellenburg, S. Laptenok, R. Seger, K. M. Mullen, I. H. M. van Stokkum, J. Stat. Software 2012, **49**, 1–22.